groups (PND 1: CB-NP, 2.00 ± 0.15 g and control, 1.94 ± 0.18 g; PND 3: CB-NP, 2.83 ± 0.36 g and control, 2.87 ± 0.29 g; PND 5: CB-NP, 3.33 ± 0.29 g and control, 3.46 ± 0.29 g; PND 14: CB-NP, 7.85 ± 1.98 g and control, 7.99 ± 0.73 g) [$F(1, 80) = 0.19$, $P = 0.66$]. Body weight of female offspring was not affected by prenatal CB-NP exposure (PND 5: CB-NP, 3.20 ± 0.43 g and control, 3.05 ± 0.39 g). No death or malformation was observed in the CB-NP exposed and control offspring mice.

Immunophenotype of lymphocytes in the spleen

The effect of CB-NP on the immunophenotypes of lymphocytes in the spleen of male pups was examined by flow cytometry. Splenic lymphocyte count was not significantly affected by CB-NP treatment in 1-, 3- and 5-day-old offspring (Fig. 2A). CB-NP significantly decreased the splenic $CD3^+$, $CD4^+$ and $CD8^+$ cells in the newborn mice (Fig. 2B-D); the counts recovered at 14 days postpartum (Supplemental Data 1). There was no significant difference in $B220^+$ cells between the groups in the newborn offspring mice (Fig. 2E, Supplemental Data 1).

mRNA expression and cytokine production

Splenic gene expression was examined for both male and female 5-day-old offspring mouse in order to investigate the sex difference in the developmental effects of CB-NP (Jackson *et al.*, 2012b). Target genes were selected from a microarray data deposited in Gene Expression Omnibus (GSE50432), which shows gene expression profile related to the effects of prenatal CB-NP exposure on the spleen. Quantitative RT-PCR showed an increase in expression level of *Il15*, which plays an important role in T cell survival (Schluns and Lefrançois, 2003), after prenatal CB-NP treatment in the spleens of male offspring (Fig. 3). Splenic expression levels of *Ccl19* and *Ccr7* were significantly increased in female offspring by prenatal CB-NP treatment (Fig. 3). In contrast, expression of splenic mRNA of *Il7*, which also encodes a cytokine regulating T cell survival (Schluns and Lefrançois, 2003) was not significantly altered (Fig. 3). To investigate the mechanism underlying the decrease in T cells in the spleens of 5-day-old offspring mice, production of IL-2, a cytokine promoting T cell proliferation, by splenocytes was examined. IL-2 production in the culture supernatant of splenocytes from 5-day-old mice was not detected (< 8 pg/ml in the culture supernatant) even after Con A-stimulation. Expression of splenic mRNAs encoding *Il7*, *Il15*, *Foxp3*, *Gata3*, and *Tbx21* in the mother mice was not influenced by CB-NP treatment (Supplemental Data 2).

DISCUSSION

This study investigated the effects of prenatal CB-NP treatment on splenic phenotypes by using a CB-NP suspension prepared without bulk agglomeration or any dispersant, and showed that treating the pregnant mothers with CB-NP decreased splenic $CD3^+$ (T) cells of newborn mice. The data indicate the effects of CB-NP exposure during early gestation before embryonic lymphoid tissue development (Blackburn and Manley, 2004). On intratracheal instillation, CB-NP can traverse the air-blood barrier through large gaps between alveolar epithelial cells (Shimada *et al.*, 2006), causing pulmonary inflammation and translocating to the mediastinal lymph nodes (Shwe *et al.*, 2005) and other extrapulmonary tissues (Kreyling *et al.*, 2002; Oberdörster *et al.*, 2002). Effects of nanoparticles administered by intranasal instillation have been also reported (Tin-Tin-Win-Shwe *et al.*, 2006; Wang *et al.*, 2009; Yokota *et al.*, 2011). The exposure route is one of the model of nanoparticle inhalation, which results in its deposition through the nasopharyngeal, tracheobronchial, and alveolar regions (Oberdörster *et al.*, 2005). Inhalation exposure to carbon nanotubes is known to suppress B cell function and may cause immunosuppression in adult mice (Mitchell *et al.*, 2009), indicating that the spleen may be a major target of carbon nanoparticles. However, the effect of maternal exposure to CB-NP on lymphoid tissues of neonates was unknown.

The spleen, a secondary lymphoid organ, plays an important role in the defense system against invading pathogens, particularly against encapsulated bacteria (Mebius and Kraal, 2005). Our data showed that T cells in the spleen were decreased by CB-NP in newborn offspring, while the body weight and total number of lymphocytes in the spleen of offspring was not influenced. Additionally, the number of both $CD4^+$ and $CD8^+$ cells were significantly decreased in the newborn offspring mouse. Neonates are not intrinsically deficient in T cells and have the capacity to mount adult-like Th1 and cytotoxic T cell responses (Adkins, 1999). Thus, a decrease in T cells as a whole may be linked to an immunosuppressed phenotype in the infantile period (Verbsky *et al.*, 2012).

Furthermore, the number of lymphocyte exponentially increases during neonatal development (Fagoaga *et al.*, 2000); therefore, it is possible that prenatal CB-NP treatment may have influenced the proliferation of lymphocyte in the offspring during the newborn period. However, mRNA expression of *Il7*, encoding a cytokine crucial for the development and homeostasis of lymphocytes (Surh and Sprent, 2008), in the spleen was not affected by CB-NP treatment. Production of IL-2, a cytokine that

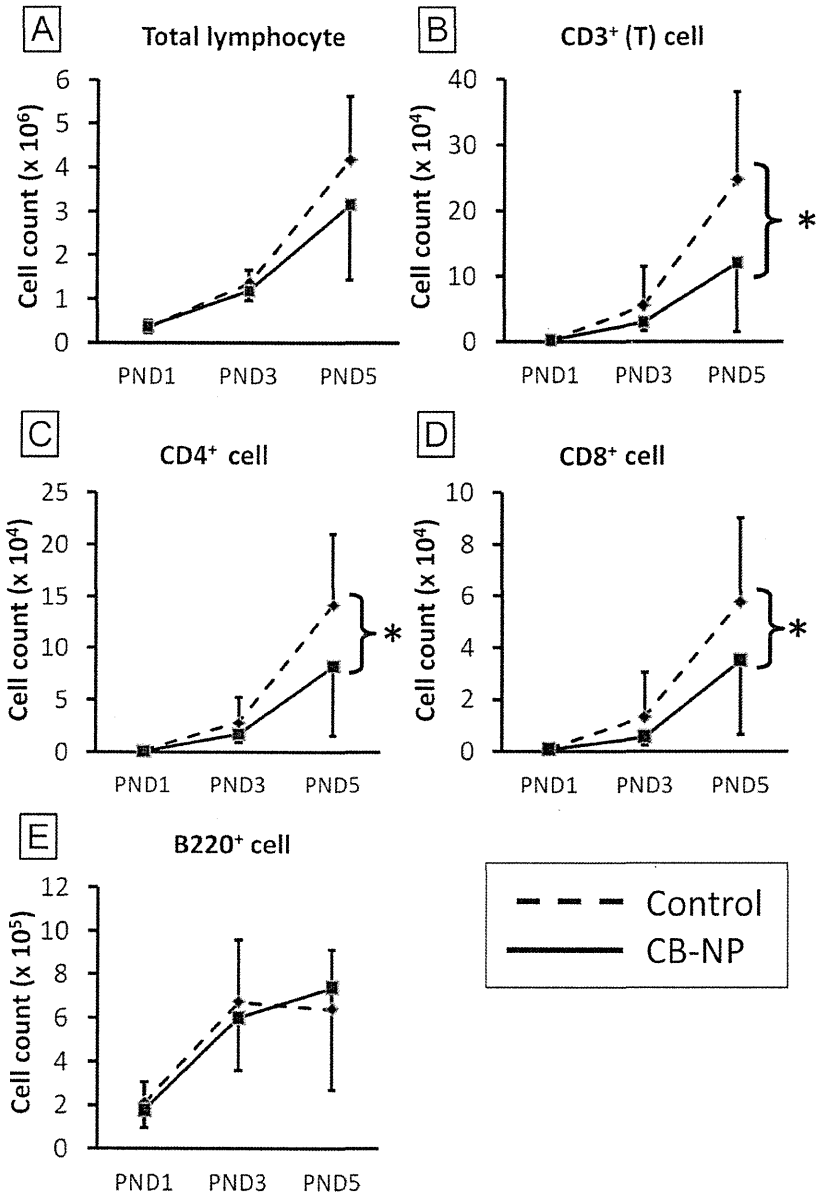

Fig. 2. Effect of maternal exposure to CB-NP on splenic lymphocyte phenotype of newborn (1-5-day old) mouse. Populations of splenic lymphocytes were analyzed by flow cytometry. Data are shown as mean ± S.D. Two-way ANOVA showed a significant main effect of CB-NP on (B) $CD3^+$ cell count [$F(1, 57) = 6.78$, $^*P < 0.05$] with CB-NP/age interaction [$F(1, 57) = 4.13$, $P < 0.05$]. *Post hoc* Tukey-Kramer's test showed that $CD3^+$ cell count was significantly decreased on PND 5 ($P < 0.001$). Two-way ANOVA also showed a significant main effect of CB-NP on (C) $CD4^+$ cell [$F(1, 56) = 5.03$, $^*P < 0.05$] and (D) $CD8^+$ cell counts [$F(1, 56) = 4.26$, $^*P < 0.05$] without CB-NP/age interaction.

is important for T cell proliferation (Boyman and Sprent, 2012), was not detected in the culture supernatant of stimulated splenocytes of 5-day-old mice in any groups. Thus, the decrease in T cells in the spleen of the exposure group was not mediated by T cell proliferation mechanism.

The decrease in T cells in the spleen had recovered by 14 days after birth. The mRNA expression profile in the spleens of 5-day-old mice provided insights into the

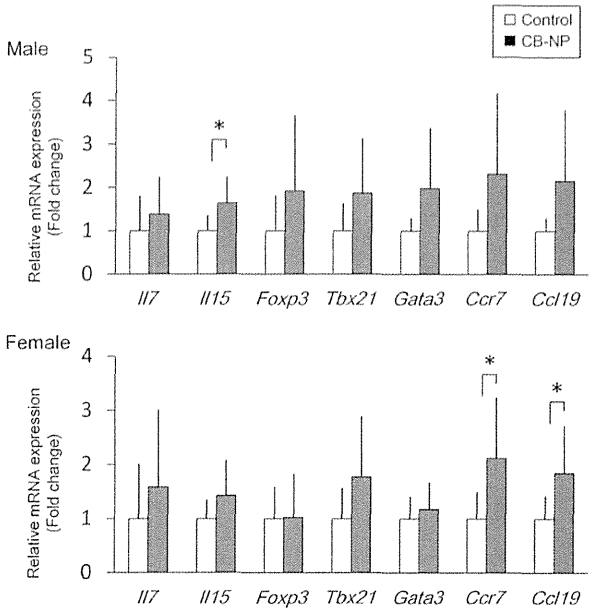

Fig. 3. Effect of maternal exposure to CB-NP on mRNA expression in the spleen of 5-day-old offspring mouse. mRNA expression levels in the spleens were examined by quantitative RT-PCR. Data are shown as mean ± SD. Data were statistically analyzed using Student's *t*-test to compare between control and CB-NP groups for each sex, and corrected with Bonferroni's method. The level of significance was set at $P < 0.05$.

mechanism of this recovery. Naive T cells continuously circulate between blood and lymphoid tissues under homeostatic conditions. T cell homing to secondary lymphoid tissue is mainly regulated by Ccr7 and its two ligands, Ccl19 and Ccl21 (Förster *et al.*, 2008). These ligands are produced only by fibroblastic reticular cells and in inflammation also by dendritic cells, and are essentially involved in the chemotaxis of various subpopulations of T cells and antigen-presenting dendritic cells to lymphoid tissues (Förster *et al.*, 2008). In our study, mRNA expression levels of *Ccl19*, *Ccr7*, and *Il15* which contributes to T cell survival in the spleen were significantly increased in 5-day-old male or female offspring mice of the treated group. Splenic mRNA change profiles by CB-NP were similar between male and female offspring. These factors may increase the migration of T cells to the spleen in 5-14 day-old offspring in the group. Because the gene expression change in the spleen did not indicate the mechanism underlying T cell decrease by prenatal CB-NP exposure, the thymus, which is an important organ for the T cell development, may be the primary target of CB-NP.

In the neonatal immune system, vigorous differential proliferation of lymphocytes occurs by weaning age, when maternal (transplacental) serum antibodies and milk-borne antibodies and cells are declining (Harris *et al.*, 2006). Hence we need to know under what circumstances there would be a positive or a negative effect on the development of the offspring's own immune system (Hasselquist and Nilsson, 2009). In the present study, no significant effect of CB-NP on the maternal immune system was observed. Whether carbon nanoparticle induces oxidative stress in biological organs remains controversial (Oberdörster, 2004; Tin-Tin-Win-Shwe *et al.*, 2006; Ryan *et al.*, 2007). CB-NPs induced apoptosis in bronchial epithelial cells *in vitro* via a ROS-dependent mitochondrial pathway (Hussain *et al.*, 2010). However, the dose of nanoparticle exerting an effect on lymphocytes in offspring mice seems to be lower than that used in previous studies. A previous study showed that single-wall carbon nanotube but no CB-NP affects placental morphology and induces oxidative stress in placenta and fetus (Pietroiusti *et al.*, 2011). Our preliminary data also indicated that the low dose of CB-NP do not increase any markers of oxidative stress in blood and tissue samples of offspring mice (data not shown). Especially, the level of 8-OHdG, an oxidative stress marker, was decreased in the lung of mothers at 21 days post-partum (Supplemental Data 3). These data indicate that the decreased number of T cells in the spleen of neonatal mice could be modified by exposure to CB-NP even in the absence of induction of oxidative stress or inflammation in the mother mice.

In conclusion, the present study showed that maternal exposure to CB-NP during early gestation decreased T cells in the spleen in newborn mice. The decrease in splenic T cells in the treated group recovered at 14 days after birth. Increased expression of splenic *Il15*, *Ccr7* and *Ccl19* may contribute to the recovery process during the infantile period. CB-NP and other nanomaterials have applications in industrial use and nanomedicine. This is the first report of developmental effect of nanoparticle on the lymphatic phenotype. The effect of nanoparticles on the neonatal immune system supports a creative approach to the development of such nanotechnology, particularly nanomedicine employing inorganic nano-sized carbon material, and also provides a method for hazard assessment of nanoparticle exposure during early pregnancy.

ACKNOWLEDGMENTS

This work was supported in part by a JSPS KAKENHI Grant Number 24790130 (Masakazu Umezawa; 2012-2013), a MEXT-Supported Program for the Strategic

Research Foundation at Private Universities (Ken Takeda; 2011-2015) and a Grant-in-Aid for the Health and Labour Sciences Research Grant (Research on the Risk of Chemical Substances) from the Ministry of Health, Labour and Welfare (Grant Number 12103301, Ken Takeda; 2012-2014). The funders had no role in the study design, data collection and analysis, decision to publish, or preparation of the manuscript. We thank Dr. Ken-ichiro Suzuki for help with the analysis of CB-NP in the suspension and valuable discussion. We also thank Mr. Rikio Niki and Ms. Rie Numazaki and the graduate and undergraduate students in the Takeda laboratory, especially Mr. Keisuke Sekita and Mr. Shotaro Matsuzawa for their technical assistance.

REFERENCES

Adkins, B. (1999): T-cell function in newborn mice and humans. Immunol. Today, **20**, 330-335.

Blackburn, C.C. and Manley, N.R. (2004): Developing a new paradigm for thymus organogenesis. Nat. Rev. Immunol., **4**, 278-289.

Boyman, O. and Sprent, J. (2012): The role of interleukin-2 during homeostasis and activation of the immune system. Nat. Rev. Immunol., **12**, 180-190.

Camacho, I.A., Nagarkatti, M. and Nagarkatti, P.S. (2004): Effect of 2,3,7,8-tetrachlorodibenzo-p-dioxin (TCDD) on maternal immune response during pregnancy. Arch. Toxicol., **78**, 290-300.

Clouser, C.L., Holtz, C.M., Mullett, M., Crankshaw, D.L., Briggs, J.E., O'Sullivan, M.G., Patterson, S.E. and Mansky, L.M. (2012): Activity of a novel combined antiretroviral therapy of gemcitabine and decitabine in a mouse model for HIV-1. Antimicrob. Agents Chemother., **56**, 1942-1948.

Ema, M., Kobayashi, N., Naya, M., Hanai, S. and Nakanishi, J. (2010): Reproductive and developmental toxicity studies of manufactured nanomaterials. Reprod. Toxicol., **30**, 343-352.

Fagoaga, O.R., Yellon, S.M. and Nehlsen-Cannarella, S.L. (2000): Maturation of lymphocyte immunophenotypes and memory T helper cell differentiation during development in mice. Dev. Immunol., **8**, 47-60.

Fedulov, A.V., Leme, A., Yang, Z., Dahl, M., Lim, R., Mariani, T.J. and Kobzik, L. (2008): Pulmonary Exposure to Particles during Pregnancy Causes Increased Neonatal Asthma Susceptibility. Am. J. Respir. Cell Mol. Biol., **38**, 57-67.

Forni, L., Heusser, C. and Coutinho, A. (1988): Natural lymphocyte activation in postnatal development of germ-free and conventional mice. Ann. Inst. Pasteur Immunol., **139**, 245-256.

Förster, R., Davalos-Misslitz, A.C. and Rot, A. (2008): CCR7 and its ligands: balancing immunity and tolerance. Nat. Rev. Immunol., **8**, 362-371.

Fukuhara, N., Suzuki, K., Takeda, K. and Nihei, N. (2008): Characterization of environmental nanoparticles. Appl. Surf. Sci., **255**, 1538-1540.

Harris, N.L., Spoerri, I., Schopfer, J.F., Nembrini, C., Merky, P., Massacand, J., Urban, J.F. Jr., Lamarre, A., Burki, K., Odermatt, B., Zinkernagel, R.M. and Macpherson, A.J. (2006): Mechanisms of neonatal mucosal antibody protection. J. Immunol., **177**, 6256-6262.

Hasselquist, D. and Nilsson, J.A. (2009): Maternal transfer of antibodies in vertebrates: trans-generational effects on offspring immunity. Philos. Trans. R. Soc. Lond. B Biol. Sci., **364**, 51-60.

Hougaard, K.S., Jackson, P., Jensen, K.A., Sloth, J.J., Löschner, K., Larsen, E.H., Birkedal, R.K., Vibenholt, A., Boisen, A.M., Wallin, H. and Vogel, U. (2010): Effects of prenatal exposure to surface-coated nanosized titanium dioxide (UV-Titan). A study in mice. Part. Fibre Toxicol., **7**, 16.

Hussain, S., Thomassen, L.C., Ferecatu, I., Borot, M.C., Andreau, K., Martens, J.A., Fleury, J., Baeza-Squiban, A., Marano, F. and Boland, S. (2010): Carbon black and titanium dioxide nanoparticles elicit distinct apoptotic pathways in bronchial epithelial cells. Part. Fibre Toxicol., **7**, 10.

Jackson, P., Halappanavar, S., Hougaard, K.S., Williams, A., Madsen, A.M., Lamson, J.S., Andersen, O., Yauk, C., Wallin, H. and Vogel, U. (2013): Maternal inhalation of surface-coated nanosized titanium dioxide (UV-Titan) in C57BL/6 mice: effects in prenatally exposed offspring on hepatic DNA damage and gene expression. Nanotoxicology, **7**, 85-96.

Jackson, P., Hougaard, K.S., Boisen, A.M., Jacobsen, N.R., Jensen, K.A., Møller, P., Brunborg, G., Gutzkow, K.B., Andersen, O., Loft, S., Vogel, U. and Wallin, H. (2012a): Pulmonary exposure to carbon black by inhalation or instillation in pregnant mice: effects on liver DNA strand breaks in dams and offspring. Nanotoxicology, **6**, 486-500.

Jackson, P., Hougaard, K.S., Vogel, U., Wu, D., Casavant, L., Williams, A., Wade, M., Yauk, C.L., Wallin, H. and Halappanavar, S. (2012b): Exposure of pregnant mice to carbon black by intratracheal instillation: toxicogenomic effects in dams and offspring. Mutat. Res., **745**, 73-83.

Jackson, P., Vogel, U., Wallin, H. and Hougaard, K.S. (2011): Prenatal exposure to carbon black (printex 90): effects on sexual development and neurofunction. Basic Clin. Pharmacol. Toxicol., **109**, 434-437.

Kannan, S., Misra, D.P., Dvonch, J.T. and Krishnakumar, A. (2007): Exposures to airborne particulate matter and adverse perinatal outcomes: a biologically plausible mechanistic framework for exploring potential. Cien. Saude Colet., **12**, 1591-1602.

Kessler, R. (2011): Engineered nanoparticles in consumer products: understanding a new ingredient. Environ. Health Perspect., **119**, 120-125.

Kreyling, W.G., Semmler, M., Erbe, F., Mayer, P., Takenaka, S., Schulz, H., Oberdörster, G. and Ziesenis, A. (2002): Translocation of ultrafine insoluble iridium particles from lung epithelium to extrapulmonary organs is size dependent but very low. J. Toxicol. Environ. Health A, **65**, 1513-1530.

Kubo-Irie, M., Uchida, H., Mastuzawa, S., Yoshida, Y., Shinkai, Y., Suzuki, K., Yokota, S., Oshio, S. and Takeda, K. (2014): Dose-dependent biodistribution of prenatal exposure to rutile-type titanium dioxide nanoparticles on mouse testis. J. Nanopart. Res., **16**, 2284.

Lamoureux, D.P., Kobzik, L. and Fedulov, A.V. (2010): Customized PCR-array analysis informed by gene-chip microarray and biological hypothesis reveals pathways involved in lung inflammatory response to titanium dioxide in pregnancy. J. Toxicol. Environ. Health A, **73**, 596-606.

Levy, O. (2007): Innate immunity of the newborn: basic mechanisms and clinical correlates. Nat. Rev. Immunol., **7**, 379-390.

Mebius, R.E. and Kraal, G. (2005): Structure and function of the spleen. Nat. Rev. Immunol., **5**, 606-616.

Mitchell, L.A., Lauer, F.T., Burchiel, S.W. and McDonald, J.D. (2009): Mechanisms for how inhaled multiwalled carbon nano-

tubes suppress systemic immune function in mice. Nat. Nanotechnol., **4**, 451-456.

Mustafa, A., Holladay, S.D., Goff, M., Witonsky, S., Kerr, R., Weinstein, D.A., Karpuzoglu-Belgin, E. and Gogal, R.M.Jr. (2009): Developmental exposure to 2,3,7,8-tetrachlorodibenzo-p-dioxin alters postnatal T cell phenotypes and T cell function and exacerbates autoimmune lupus in 24-week-old SNF1 mice. Birth Defects Res. A Clin. Mol. Teratol., **85**, 828-836.

Oberdörster, E. (2004): Manufactured nanomaterials (fullerenes, C_{60}) induce oxidative stress in the brain of juvenile largemouth bass. Environ. Health Perspect., **112**, 1058-1062.

Oberdörster, G., Oberdörster, E. and Oberdörster, J. (2005): Nanotoxicology: an emerging discipline evolving from studies of ultrafine particles. Environ. Health Perspect., **113**, 823-839.

Oberdörster, G., Sharp, Z., Atudorei, V., Elder, A., Gelein, R., Lunts, A., Kreyling, W. and Cox, C. (2002): Extrapulmonary translocation of ultrafine carbon particles following whole-body inhalation exposure of rats. J. Toxicol. Environ. Health A, **65**, 1531-1543.

Onoda, A., Umezawa, M., Takeda, K., Ihara, T. and Sugamata, M. (2014). Effects of maternal exposure to ultrafine carbon black on brain perivascular macrophages and surrounding astrocytes in offspring mice. PLoS One, in press.

Pietroiusti, A., Massimiani, M., Fenoglio, I., Colonna, M., Valentini, F., Palleschi, G., Camaioni, A., Magrini, A., Siracusa, G., Bergamaschi, A., Sgambato, A. and Campagnolo, L. (2011): Low doses of pristine and oxidized single-wall carbon nanotubes affect mammalian embryonic development. ACS Nano, **5**, 4624-4633.

Ryan, J.J., Bateman, H.R., Stover, A., Gomez, G., Norton, S.K., Zhao, W., Schwartz, L.B., Lenk, R. and Kepley, C.L. (2007): Fullerene nanomaterials inhibit the allergic response. J. Immunol., **179**, 665-672.

Sadauskas, E., Wallin, H., Stoltenberg, M., Vogel, U., Doering, P., Larsen, A. and Danscher, G (2007): Kupffer cells are central in the removal of nanoparticles from the organism. Part. Fibre Toxicol., **4**, 10.

Schluns, K.S. and Lefrançois, L. (2003): Cytokine control of memory T-cell development and survival. Nat. Rev. Immunol., **3**, 269-279.

Shimada, A., Kawamura, N., Okajima, M., Kaewamatawong, T., Inoue, H. and Morita, T. (2006): Translocation pathway of the intratracheally instilled ultrafine particles from the lung into the blood circulation in the mouse. Toxicol. Pathol., **34**, 949-957.

Shimizu, M., Tainaka, H., Oba, T., Mizuo, K., Umezawa, M. and Takeda, K. (2009): Maternal exposure to nanoparticulate titanium dioxide during the prenatal period alters gene expression related to brain development in the mouse. Part. Fibre Toxicol., **6**, 20.

Shwe, T.T., Yamamoto, S., Kakeyama, M., Kobayashi, T. and Fujimaki, H. (2005): Effect of intratracheal instillation of ultrafine carbon black on proinflammatory cytokine and chemokine release and mRNA expression in lung and lymph nodes of mice. Toxicol. Appl. Pharmacol., **209**, 51-61.

Surh, C.D. and Sprent, J. (2008): Homeostasis of naive and memory T cells. Immunity, **29**, 848-862.

Takahashi, Y., Mizuo, K., Shinkai, Y., Oshio, S. and Takeda, K. (2010): Prenatal exposure to titanium dioxide nanoparticles increases dopamine levels in the prefrontal cortex and neostriatum of mice. J. Toxicol. Sci., **35**, 749-756.

Takeda, K., Suzuki, K., Ishihara, A., Kubo-Irie, M., Fujimoto, R., Tabata, M., Oshio, S., Nihei, Y., Ihara, T. and Sugamata, M. (2009): Nanoparticles transferred from pregnant mice to their offspring can damage the genital and cranial nerve systems. J. Health Sci., **55**, 95-102.

Tasker, L., Lindsay, R.W., Clarke, B.T., Cochrane, D.W. and Hou, S. (2008): Infection of mice with respiratory syncytial virus during neonatal life primes for enhanced antibody and T cell responses on secondary challenge. Clin. Exp. Immunol., **153**, 277-288.

Tin-Tin-Win-Shwe, Yamamoto, S., Ahmed, S., Kakeyama, M., Kobayashi, T. and Fujimaki, H. (2006): Brain cytokine and chemokine mRNA expression in mice induced by intranasal instillation with ultrafine carbon black. Toxicol. Lett., **163**, 153-160.

Umezawa, M., Kudo, S., Yanagita, S., Shinkai, Y., Niki, R., Oyabu, T., Takeda, K., Ihara, T. and Sugamata, M. (2011): Maternal exposure to carbon black nanoparticle increases collagen type VIII expression in the kidney of offspring. J. Toxicol. Sci., **36**, 461-468.

Umezawa, M., Tainaka, H., Kawashima, N., Shimizu, M. and Takeda, K. (2012): Effect of fetal exposure to titanium dioxide nanoparticle on brain development - brain region information. J. Toxicol. Sci., **37**, 1247-1252.

Verbsky, J.W., Baker, M.W., Grossman, W.J., Hintermeyer, M., Dasu, T., Bonacci, B., Reddy, S., Margolis, D., Casper, J., Gries, M., Desantes, K., Hoffman, G.L., Brokopp, C.D., Seroogy, C.M. and Routes, J.M. (2012): Newborn Screening for Severe Combined Immunodeficiency; The Wisconsin Experience (2008-2011). J. Clin. Immunol., **32**, 82-88.

Wang, B., Feng, W., Zhu, M., Wang, Y., Wang, M., Gu, Y., Ouyang, H., Wang, H., Li, M., Zhao, Y., Chai, Z. and Wang, H. (2009): Neurotoxicity of low-dose repeatedly intranasal instillation of nano- and submicron-sized ferric oxide particles in mice. J. Nanopart. Res., **11**, 41-53.

Watanabe, M., Nakajima, S., Ohnuki, K., Ogawa, S., Yamashita, M., Nakayama, T., Murakami, Y., Tanabe, K. and Abe, R. (2012): AP-1 is involved in ICOS gene expression downstream of TCR/CD28 and cytokine receptor signaling. Eur. J. Immunol., **42**, 1850-1862.

Wick, P., Malek, A., Manser, P., Meili, D., Maeder-Althaus, X., Diener, L., Diener, P.A., Zisch, A., Krug, H.F. and von Mandach, U. (2010): Barrier capacity of human placenta for nanosized materials. Environ. Health Perspect., **118**, 432-436.

Yamashita, K., Sakai, M., Takemoto, N., Tsukimoto, M., Uchida, K., Yajima, H., Oshio, S., Takeda, K. and Kojima, S. (2009): Attenuation of delayed-type hypersensitivity by fullerene treatment. Toxicology, **261**, 19-24.

Yamashita, K., Yoshioka, Y., Higashisaka, K., Mimura, K., Morishita, Y., Nozaki, M., Yoshida, T., Ogura, T., Nabeshi, H., Nagano, K., Abe, Y., Kamada, H., Monobe, Y., Imazawa, T., Aoshima, H., Shishido, K., Kawai, Y., Mayumi, T., Tsunoda, S., Itoh, N., Yoshikawa, T., Yanagihara, I., Saito, S. and Tsutsumi, Y. (2011): Silica and titanium dioxide nanoparticles cause pregnancy complications in mice. Nat. Nanotechnol., **6**, 321-328.

Yokota, S., Takashima, H., Ohta, R., Saito, Y., Miyahara, T., Yoshida, Y., Negura, T., Senuma, M., Usumi, K., Hirabayashi, N., Watanabe, T., Horiuchi, S., Fujitani, Y., Hirano, S. and Fujimaki, H. (2011): Nasal instillation of nanoparticle-rich diesel exhaust particles slightly affects emotional behavior and learning capability in rats. J. Toxicol. Sci., **36**, 267-276.

Yoshida, S., Hiyoshi, K., Oshio, S., Takano, H., Takeda, K. and Ichinose, T. (2010). Effects of fetal exposure to carbon nanoparticles on reproductive function in male offspring. Fertil. Steril., **93**, 1695-1699.

Toxicology 321 (2014) 13–20

Contents lists available at ScienceDirect

Toxicology

journal homepage: www.elsevier.com/locate/toxicol

Purinergic signaling via $P2X_7$ receptor mediates IL-1β production in Kupffer cells exposed to silica nanoparticle

Shuji Kojima[a,*], Yusuke Negishi[a], Mitsutoshi Tsukimoto[a], Takato Takenouchi[c], Hiroshi Kitani[c], Ken Takeda[b]

[a] Department of Radiation Biosciences, Faculty of Pharmaceutical Sciences, Tokyo University of Science (TUS), 2641 Yamazaki, Noda-shi, Chiba 278-8510, Japan
[b] Department of Hygienic Chemistry, Faculty of Pharmaceutical Sciences, Tokyo University of Science (TUS), 2641 Yamazaki, Noda-shi, Chiba 278-8510, Japan
[c] Transgenic Animal Research Center, National Institute of Agrobiological Sciences, Ohwashi 1-2, Tsuuba, Ibaraki 305-8634, Japan

ARTICLE INFO

Article history:
Received 25 February 2014
Received in revised form 20 March 2014
Accepted 21 March 2014
Available online 28 March 2014

Keywords:
Silica nanoparticle
Kupffer cell
IL-1β
Inflammasome
ATP
$P2X_7$ receptor

ABSTRACT

There is extensive evidence that nanoparticles (NPs) cause adverse effects in multiple organs, including liver, though the mechanisms involved remain to be fully established. Kupffer cells are macrophages resident in the liver, and play important roles in liver inflammation induced by various toxic agents, including lipopolysaccharide (LPS). Interleukin-1 (IL-1) family members IL-1α,β are released from LPS-primed macrophages exposed to NPs, including silica NPs (SNPs), via activation of nucleotide-binding oligomerization domain-like receptor family pyrin domain-containing 3 inflammasomes. Here, we investigated the mechanism of production of IL-1β via activation of inflammasomes in mouse Kupffer cell line KUP5, focusing on the role of purinergic signaling via $P2X_7$ receptor.

IL-1β production by LPS-primed KUP5 cells exposed to SNPs was increased dose-dependently, and was greatest in response to SNPs with a diameter of 30 nm (SNP30), as compared with 70-nm and 300-nm SNPs (SNP70 and SNP300). ATP release was also highest in cells exposed to SNP30. Treatment of LPS-primed KUP5 cells with ATP also induced a high level of IL-1β production, similar to that induced by SNP30. IL-1β production was significantly inhibited by apyrase (an ecto-nucleotidase) and A438079 (a $P2X_7$ antagonist/ATP-release inhibitor). Production of reactive oxygen species (ROS) was confirmed in cells exposed to SNP30.

In conclusion, ATP released from $P2X_7$ receptor in response to stimulation of KUP5 cells with SNP30 induces ROS production via cell-membrane NADPH oxidase. The ROS causes activation of inflammasomes, leading to caspase-1-dependent processing of IL-1β.

1. Introduction

Various types of nanoparticles (NPs) with novel electrical, catalytic, magnetic, mechanical, photonic and thermal properties, have been developed and are already in use or are being tested in a wide range of consumer products, including sunscreens, composites, and medical and electronic devices. Specific properties of NPs, such as their small size, shape, high surface area, and special structure, make these compounds promising candidates for industrial and biological applications (Luo et al., 2006; Yang et al., 2008; Uskoković, 2013; Zhang et al., 2013). However, there is increasing evidence of adverse effects of NPs (Aillon et al., 2009; Borm and Kreyling, 2004; Crosera et al., 2009; Donaldson et al., 2005; Medina et al., 2007; Xia et al., 2006). There have been extensive human health and environmental safety investigations of commercially available NPs, such as silica, titanium oxide (TiO_2), silver, chrysotile asbestos, carbon nanotubes, and some magnetic particles, in *in vitro* and *in vivo* experimental systems. Exposure to NP is likely to occur through inhalation, dermal contact, or injection. NPs are then transferred to blood, and may cause adverse effects in various organs, including liver, spleen, lungs, kidneys, testis and brain. Silica NPs (SNPs) in particular have found extensive applications in various fields, e.g., as additives in cosmetics, medical supplies, printer toners, and foods. Nevertheless, there is increasing concern about their possible effects on human health (Napierska et al., 2010). The liver is a primary target organ for NPs, including SNPs. It has been shown

* Corresponding author. Tel.: +81 47121 3613; fax: +81 47121 3613.
E-mail address: kjma@rs.noda.tus.ac.jp (S. Kojima).

http://dx.doi.org/10.1016/j.tox.2014.03.008
0300-483X/

that SNPs induce liver injury both directly and indirectly (Chen et al., 2013; Hasezaki et al., 2011; Isoda et al., 2013; Liu et al., 2012; Yu et al., 2013).

Kupffer cells are macrophages resident in the liver, and are involved in immune functions such as phagocytosis and antigen-presenting ability, leading to induction of regeneration, fibrogenesis, inflammation, and necrosis (Kolios et al., 2006). They also participate in the acute and chronic responses of the liver to toxic agents (Laskin and Pilaro, 1986; Thakur et al., 2007; West et al., 1989; Winwood and Arthur, 2006), which activate these cells, leading to hepatic damage through the release of toxic molecules, such as radical oxygen species (ROS) and pro-inflammatory cytokines (Feder et al., 1993; Laskin et al., 1988; Liu et al., 2010; McCloskey et al., 1992; Michael et al., 1999; Pilaro and Laskin, 1986; Yee et al., 2003). Recent reports show that interleukin-1 family members IL-1α,β are released from LPS-primed macrophages exposed to certain NPs, including SNPs, via activation of nucleotide-binding oligomerization domain-like receptor (NLR) family pyrin domain-containing 3 (NLRP3) inflammasomes (Deng et al., 2011; Morishige et al., 2010; Reisetter et al., 2011; Sandberg et al., 2012; Schanen et al., 2009; Winter et al., 2011; Yazdi et al., 2010).

Nucleotides, such as ATP and UTP, are physiologically released from cytoplasm into the extracellular space in various types of cells both under basal conditions and in response to various stimuli (Burnstock, 2007, 2014; Corriden and Insel, 2010; Lazarowski et al., 2011). Extracellular ATP, in particular, plays an important role in rapid intracellular signaling. These nucleotides bind to specific plasma membrane receptors called purinergic (P2) receptors, and immediately activate them (Bodin and Burnstock, 2001; Yegutkin, 2008). Two large families of P2 receptors are known, ligand-gated ionotropic $P2X_{1-7}$ receptors and G-protein-coupled metabotropic $P2Y_{1,2,4,6,11-14}$ receptors (Burnstock, 2014). Released ATP is rapidly degraded to ADP (an agonist of P2Y receptors), AMP and adenosine (an agonist of P1 receptors) by ecto-nucleotidase (Yegutkin, 2008; Lazarowski et al., 2003). The $P2X_7$ receptor is unique among P2X receptors in that it is activated by LPS and other inflammatory stimuli, leading to Ca^{2+} influx (Bianchi et al., 1999), non-selective pore (non-selective channel) opening (Surprenant et al., 1996), ROS production via activation of NADPH oxidase (Noguchi et al., 2008; Ohshima et al., 2011; Suh et al., 2001), IL-1β release (Ferrai et al., 2006; Humphreys and Dubyak, 1998), and cell death (Tsukimoto et al., 2006). Since the non-selective $P2X_7$ channel allows the passage of hydrophilic molecules with a size of 400–900 Da, it provides a route for release of ATP (MW: 507 Da) from cells (Di Virgilio et al., 1998; Ohshima et al., 2010; Surprenant et al., 1996).

The extracellular ATP-gated cation channel $P2X_7$ is an important upstream activator of inflammasomes (Franchi et al., 2012; Pelegrin and Surprenant, 2006; Riteau et al., 2010; Zambetti et al., 2012). More recently, participation of ATP in the activation of NLRP3 inflammasomes by NPs has also been suggested, and it was shown that uric acid, silica, and alum particles induce active release of intracellular ATP from human macrophages to the extracellular compartment via mechanisms dependent upon purinergic signaling (Riteau et al., 2012). However, the precise mechanism of $P2X_7$ receptor-mediated purinergic signaling involved in activation of NLRP3, leading to IL-1β release, is unclear. In this study, we investigated the mechanism of IL-1β production induced by SNPs in LPS-primed mouse Kupffer cell line KUP5, focusing on the role of purinergic signaling via activation of $P2X_7$ receptor.

2. Materials and methods

2.1. Reagents

SNP with diameters of 30, 70, and 300 nm (designated as SNP30, SNP70 and SNP300) were purchased from Micromod Partikeltechnologie GmbH. High-glucose type Dulbecco's modified Eagle's medium (DMEM containing 4.5 g glucose/L), low-glucose type (DMEM containing 1.0 g glucose/L), F12 medium, penicillin, streptomycin, and ascorbic acid (Asc) were purchased from Wako Pure Chemical Industries (Osaka, Japan). ATP, apyrase (an ecto-nucleotidase), diphenyleneiodonium chloride (an inhibitor of NADPH-oxidase, DPI) were purchased from Sigma–Aldrich (St Louis, MO). Fetal bovine serum (FBS) was obtained from Biowest (Nuaillé, France). A438079 (a selective antagonist of $P2Y_7$) was obtained from Tocris Bioscience (Bristol, UK). All other chemicals used were of the highest purity available.

2.2. Characterization of silica NPs

The particle size distribution of SNP30, SNP70, and SNP300 in DMEM was evaluated by dynamic light-scattering (DLS), using NICOMP 370 (Particle Sizing System, Co., Tokyo, Japan). Briefly, 2.5 mg of each SNP was suspended in 1 mL low-glucose type DMEM, mixed thoroughly with vortex mixture, and immediately subjected to DLS analysis at room temperature. Morphology of SNPs prepared by the same method was assessed at room temperature by transmission electron microscopy (TEM), using a JEOL JEM 2010 (JEOL Ltd, Tokyo, Japan). Each SNP suspended in low-glucose type DMEM was dropped on the 400 mesh grid coated with carbon membrane, kept for 2 h at 37 °C, and then dried. The dried SNP was observed by TEM.

2.3. Isolation and cultivation of mouse liver Kupffer cells

Liver macrophages/Kupffer cells were isolated from mixed primary culture of C57BL/6 mouse liver cells as described, and immortalized by retroviral transduction of human *c-myc* (Kitani et al., 2011; Takenouchi et al., 2005). The clonal Kupffer cell line (KUP5) was cultivated with Dulbecco's modified Eagle's medium (high glucose type), containing 10% FBS, 100 units/mL penicillin, 100 μg/mLstreptomycin, insulin (10 μg/mL), and 2-mercaptoethanol (100 μM) in an atmosphere of 5% CO_2, 95% air at 37 °C. In most experiments, cells were seeded on Plates 24 h before stimulation with LPS (1 μg/mL).

2.4. Assay of IL-β

KUP5 cells cultivated with DMEM for 24 h were stimulated with LPS (1 μg/mL) for 4 h, and then exposed to SNPs. The culture supernatants were collected and the concentration of IL-1β was measured by enzyme-linked immunosorbent assay as described below. A 96-well plate was coated with purified anti-mouse IL-1β mAb (1:250) (eBioscience) and incubated overnight at 4 °C. The plate was washed with phosphate-buffered saline (PBS) containing 0.05% Tween 20. PBS containing 1% BSA was added, and the plate was incubated at room temperature to block non-specific binding, then washed, and the supernatants were added. Incubation was continued for 2 h at room temperature. The plate was washed again, and biotin-conjugated anti-mouse IL-1β mAb (1:500) (eBioscience) was added for 1 h at room temperature. The plate was washed, and avidin-horseradish peroxidase (Sigma) was added for 30 min at room temperature. The plate was further washed, and 3,3′,5,5′-tetramethylbenzidine was added to stain the cells. After a few minutes, the reaction was stopped by adding 2.5 M H_2SO_4. The absorbance at 450 nm was measured with a Wallac 1420 ARVO Fluoroscan (Wallac, Turku, Finland). In an experiment concerning the effects of DPI and Asc on SNP30-induced IL-1β production, LPS-primed KUP5 cells were pretreated with DPI (100 μM) or ascorbic acid (Asc, 1 mM) for 30 min before exposure to SNP30 at a concentration of 10 μg/cm². The concentration of IL-1β was estimated by interpolation on the standard curve. Pre-treatments and post-treatments with reagents were carried out at the indicated times.

2.5. Assay of cell viability

A colorimetric assay with WST-1 reagent was used to evaluate cell viability in accordance with the manufacturer's directions. KUP5 cells (1×10^5/mL) were primed for 4 h with LPS (1 μg/mL) and then exposed to different concentrations ranging from 1 to 30 μg/cm² of SNP30, SNP70 and SNP300 for 24 h. Then 10 μL of WST-1 reagent, diluted 4-fold in phosphate buffer, was added to each well and incubation was continued for another 4 h at 37 °C. The absorbance of the wells at 450 nm was measured with a plate reader. Relative cell viability was calculated as a percentage of the control group, to which SNPs had not been added.

2.6. Assay of extracellular ATP

Extracellular ATP concentration was measured using ENLITEN® Luciferase/Luciferin Reagent (Promega, Madison, WI). KUP5 cells (3.0×10^5 cells/well) were incubated in 500 μL of RPMI1640 medium containing 1% FBS for 16 h in a 12-well culture plate. For investigation of SNPs-induced ATP release, an aliquot (40 μL) of the conditioned medium was collected as a control sample for background ATP release. The cells were then incubated with SNPs for the indicated time. After incubation, 40 μL of conditioned medium was collected at the indicated time points. Each sample was centrifuged at 600 × *g* for 5 min and 10 μL of the supernatant was used for ATP determination. The concentration of ATP was determined by measuring chemiluminescence with a TR717™ Microplate Luminometer (Applied Biosystems, Foster City, CA) 1.6 s after adding 100 μL of luciferin–luciferase reagent to 10 μL of sample solution.

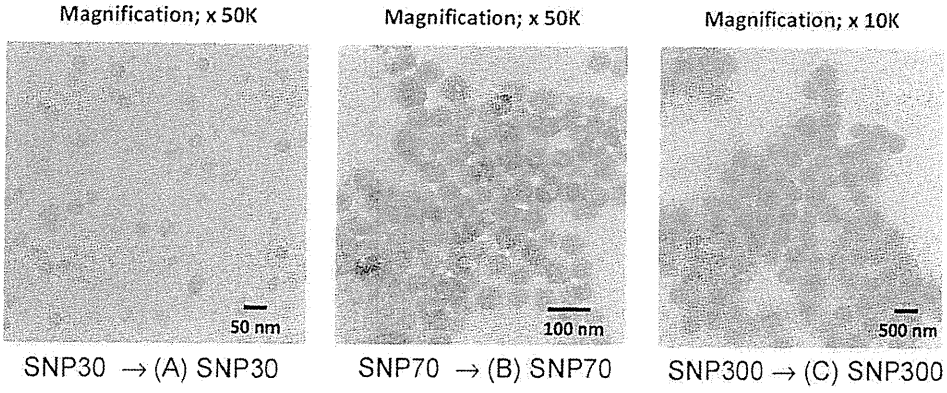

Fig. 1. Characteristics of silica nanoparticles (SNPs) observed by transmission electron microscopy. Micrographs of SNP 30 (A), SNP70 (B), and SNP300 (C) in high-glucose type DMEM. Scale bars: 50, 100 or 500 nm, as indicated.

2.7. Immunoblotting

LPS-primed KUP5 cells were dissolved in sample buffer (25% glycerin, 1% SDS, 62.5 mM Tris–Cl, 10 mM DTT) and boiled for 5 min. Aliquots of samples containing 10 μg of protein were analyzed by 15% SDS-PAGE and transferred onto a PVDF membrane. Blots were incubated at 4 °C overnight in TBST with 1% BSA, and then with rabbit anti-cleaved IL-1β antibody (1:1000) (Cell Signaling Technology, Inc., Beverly, MA), anti-mouse pro-IL1β antibody (1:1000) (Cell Signaling Technology, Inc., Beverly, MA), or mouse anti-actin antibody (1:200) (Santa Cruz Biotechnology, Santa Cruz, CA) at room temperature for 1.5 h. After having been washed with TBST, blots were incubated with goat HRP-conjugated anti-rabbit IgG antibody (1:20,000) (Cell Signaling Technology) or goat HRP-conjugated anti-mouse IgG antibody (1:20,000) (Santa Cruz Biotechnology) for 1.5 h at room temperature. The blots were further washed with TBST, and specific proteins were visualized by using ECL Western blotting detection reagents (GE Healthcare, Piscataway, NJ).

2.8. Determination of intracellular reactive oxygen species (ROS)

Intracellular ROS levels were monitored by using the fluorescent dye 2′,7′-dichloro-dihydrofluorescein diacetate (H_2DCFDA). KUP5 cells (1.0×10^5/well) were incubated in RPMI1640 medium containing 1% FBS for 24 h in a 96-well culture plate. Then, the supernatant was removed and the cells were further incubated in RPMI1640 medium containing 10 μM H_2DCFDA for 30 min. The cells were washed twice with DMEM, and exposed to SNPs (10 μg/cm^2). DCF fluorescence was monitored for 10 min with a Wallac 1420 ARVO-SX multi-label counter (Perkin-Elmer, Yokohama, Japan) (excitation/emission = 485 nm/535 nm). For the study on inhibition of SNP30-induced ROS generation, cells were pre-treated with DPI (100 μM) or A438079 (50 μM) for 30 min before exposure to SNP30 at a concentration of 10 μg/cm^2.

2.9. Statistics

Results are expressed as the mean ± S.E.M. The statistical significance of differences between two groups was calculated by using the unpaired Student's *t*-test. The statistical significance of differences between control and other groups was calculated by using Dunnett's test. The criterion of significance was $P < 0.05$ as determined with the Instat version 3.0 statistical package (Graph Pad Software, San Diego, CA).

3. Results

3.1. Characterization of silica NPs

Since NPs often agglomerate in solution, the sizes of SNP30, SNP70, and SNP300 suspended in DMEM were estimated using TEM and dynamic light scattering (DLS) measurements. As shown in Fig. 1A–C, TEM micrographs revealed that the majority of SNP30 particles had a primary particle size of <50 nm and were approximately uniformly dispersed in high-glucose type DMEM. On the other hand, the particles of SNP70 and SNP300 appeared to be loosely aggregated. The results of DLS (not shown) indicated that the average sizes of SNP30, SNP70 and SNP300 were 35.1 nm, 65.6 nm and 278.7 nm, respectively, in low-glucose type DMEM and were 34.3 nm, 230.0 nm and 309 nm, respectively, in high-glucose type DMEM.

3.2. Dose- and size-dependence of the effects of SNPs on IL-1β production and cell viability in LPS-primed KUP5 cells

First, the effects of SNP30, SNP70 and SNP300 on IL-1β production by LPS-primed KUP5 cells were examined at 24 h post-exposure. As shown in Fig. 2A, IL-1β production was increased dose-dependently by all SNPs. SNP30 induced the greatest increase ($P < 0.001$ at the dose of 10 μg/cm^2 or more).

Second, KUP5 cells were incubated for 4 h with LPS and then exposed to various concentrations of SNP30. Cleaved mature IL-1β was detected by western blotting. As shown in Fig. 2B, mature IL-1β was released from LPS-primed KUP5 cells exposed to SNP30 (1–10 μg/cm^2) in a dose-dependent manner.

Third, the time-dependence of the effect was examined with SNP30 at a fixed dose of 10 μg/cm^2. As shown in Fig. 2C, the release of IL-1β was increasing during 24 h.

Finally, the effects of SNP30, SNP70 and SNP300 on the viability of LPS-primed KUP5 cells were examined at 24 h post-treatment by means of WST-1 assay. As shown in Fig. 2D, the viability was dose-dependently reduced by all SNPs. The greatest reduction was observed in KUP5 cells exposed to SNP30 at the dose 10 μg/cm^2 or more. Interestingly, the effect of SNP70 on viability was similar to that of SNP300. This might be due to specific aggregation behavior of SNP70, since DLS analysis gave an average size of about 230 nm for SNP70, as compared with 309 nm for SNP300, in high-glucose type DMEM.

3.3. Dose- and time-dependence of the effects of SNPs on ATP release from LPS-primed KUP5 cells

The time-dependence of the effect of SNP on ATP release from LPS-primed KUP5 cells was examined with SNP30 at the fixed dose of 10 μg/cm^2. As shown in Fig. 3A, the release was significantly increased 20 min post-treatment, reached a maximum at 25 min, and thereafter declined.

Next, ATP release was compared among SNP30, SNP70 and SNP300 at 25 min post-treatment. As shown in Fig. 3B, significant release was obtained with SNP30 at the dose of 5 μg/cm^2 or more.

3.4. Effect of ATP on IL-1β production by LPS-primed KUP5 cells

Since IL1β production closely paralleled ATP release, we hypothesized that extracellular ATP plays a role in IL-1β production by LPS-primed KUP5 cells. Thus, we examined the effect of ATP on IL-1β production by LPS-primed KUP5 cells. As shown in Fig. 4A, IL-1β production was increased by 1 mM ATP to the same extent as by SNP30 at the dose of 10 μg/cm^2. Furthermore, apyrase (an ecto-nucleotidase) and A438079 (a $P2X_7$ antagonist/ATP-release

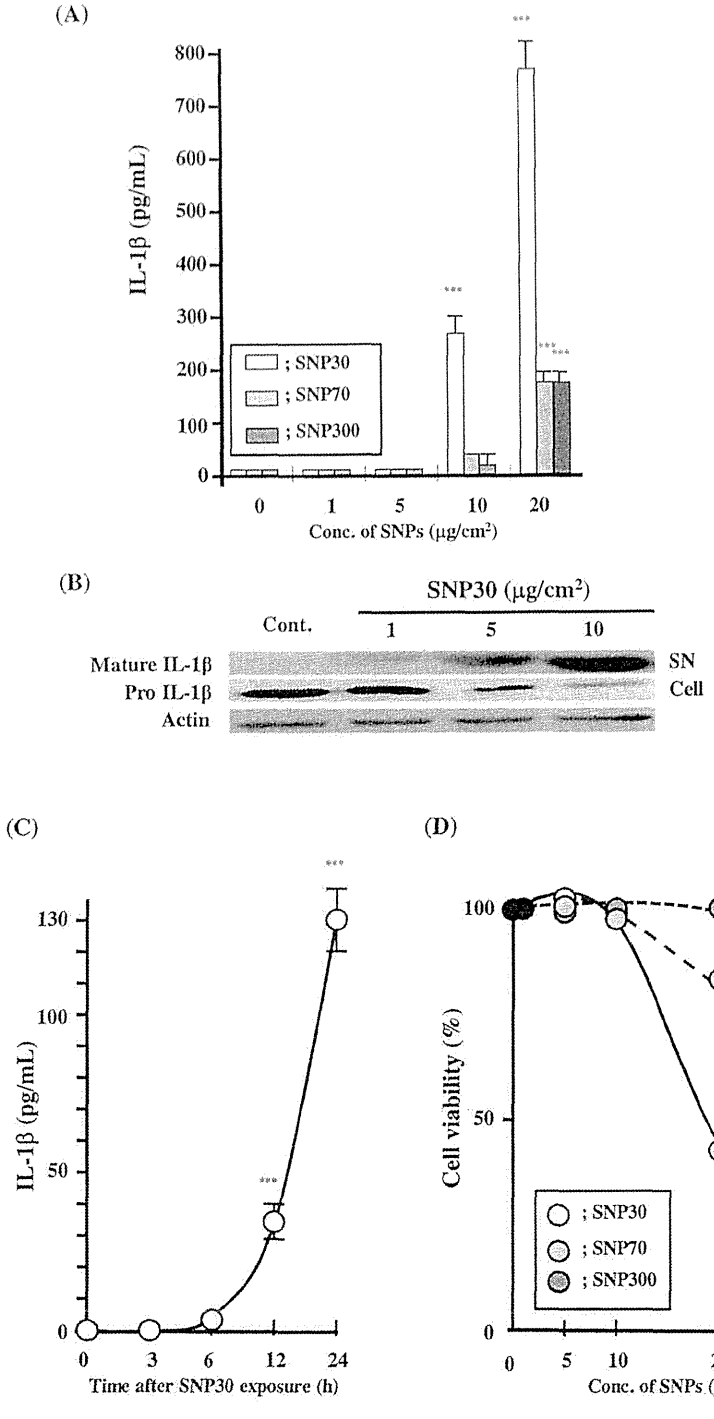

Fig. 2. Dose- and time-dependence of the effects of SNPs on IL-1β production and viability of LPS-primed KUP5 cells. (A) Dose-dependence of SNP30-, SNP70-, and SNP300-induced IL-β production. Cultivated KUP5 cells were stimulated with LPS (1 μg/mL) for 4 h, and then exposed to SNPs for 24 h at concentrations ranging from 1 μg/cm² to 20 μg/cm². The culture supernatants were collected and the concentration of IL-1β was measured by enzyme-linked immunosorbent assay. Each value represents the mean ± S.E.M. of 4 independent assays. ***$P < 0.001$ vs. each SNP conc. 0 (μg/cm²) group. (B) Dose-dependence of the effect of SNP30 on IL-1β secretion. Cultivated KUP5 cells were stimulated with LPS (1 μg/mL) for 4 h, and then treated with SNP30 at doses of 1, 5 and 10 μg/cm² for 24 h. The cell culture supernatants were concentrated and IL-1β expression was analyzed by Western blotting with anti-mouse mature IL-1β antibody (1:250) and anti-mouse pro-IL1β antibody. SN; Culture supernatant, Cell; Whole cell. (C) Time-dependence of SNP30-induced IL-β production. Cultivated KUP5 cells were stimulated with LPS (1 μg/mL) for 4 h, and then exposed to SNP30 at a fixed dose of 10 μg/cm² for the indicated time. The culture supernatant was collected at each time point and the concentration of IL-1β was measured by enzyme-linked immunosorbent assay. Each value represents the mean ± S.E.M. of 4 independent assays. ***$P < 0.001$ vs. the 0 h time point. (D) Effect of SNPs on cell viability. KUP5 cells (1×10^5/mL) were primed for 4 h with LPS (1 μg/mL) and then exposed to SNP30, SNP70, or SNP300 in the concentration range from 1 to 30 μg/cm² for 24 h. Then 10 μL of WST-1 reagent was added to each well and incubation was continued for 4 h at 37 °C. The absorbance of each well at 450 nm was measured with a plate reader. Relative cell viability was calculated as a percentage with respect to the control group (no SNP added).

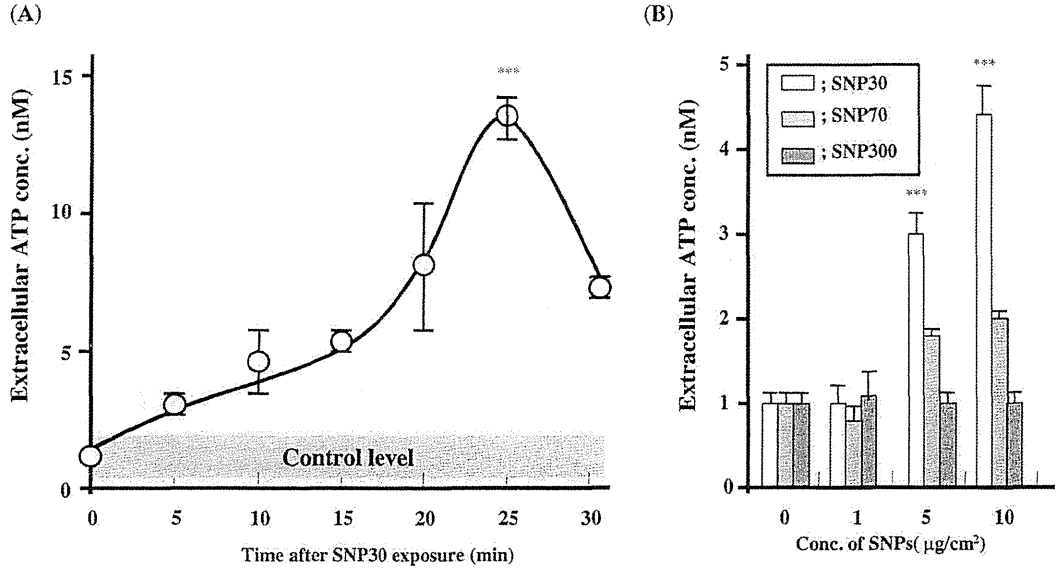

Fig. 3. Time- and dose-dependence of the effects of SNPs on extracellular ATP level of LPS-primed KUP5 cells. (A) Time-dependence of the effect of SNP30 on extracellular ATP level in KP5 cells. Cultivated KUP5 cells were stimulated with LPS (1 μg/mL) for 4 h, and then exposed to SNP30 at 10 μg/cm² for the indicated time. After incubation, the concentration of ATP in the culture medium was measured by means of luciferin/luciferase assay. Each value represents the mean ± S.E.M. of 4 independent assays. ***$P < 0.001$ vs. the 0 h time point. (B) Dose-dependence of the effects of SNP30, SNP70, and SNP300 on extracellular ATP level in KUP5 cells. Cultivated KUP5 cells were stimulated with LPS (1 μg/mL) for 4 h, and then exposed to SNPs for 25 min at 0, 1, 5 and 10 μg/cm². After incubation, the concentration of ATP in the culture medium was measured by means of luciferin/luciferase assay. Each value represents the mean ± S.E.M. of 4 independent assays. ***$P < 0.001$ vs. each SNP conc. 0 (μg/cm²) group.

inhibitor) significantly inhibited SNP30-induced IL-1β production (Fig. 4B), strongly supporting the involvement of ATP in IL-1β production by LPS-primed Kupffer cells.

3.5. Effect of SNPs on ROS production by KUP5 cells

ROS production by KUP5 cells was examined by using fluorescence reagent H_2DCFDA. First, we compared ROS production induced by SNP30, SNP70 and SNP300. As shown in Fig. 5A, only SNP30 induced significant ROS production. As shown in Fig. 5B, the increase was blocked by A438079 (50 μM) and DPI (a NADPH-oxidase inhibitor, 100 μM). These results may indicate that SNP30 causes ATP release via the non-selective channel $P2X_7$, leading to activation of P2 receptors, followed by ROS production via membrane NADPH oxidase in Kupffer cells.

3.6. Inhibitory effect of antioxidant and DPI on IL-1β production in LPS-primed KUP5 cells

The inhibitory effects of antioxidant (ascorbic acid; Asc) and NADPH oxidase inhibitor (DPI) on IL-1β production were confirmed. As shown in Fig. 6, DPI (100 μM) almost completely

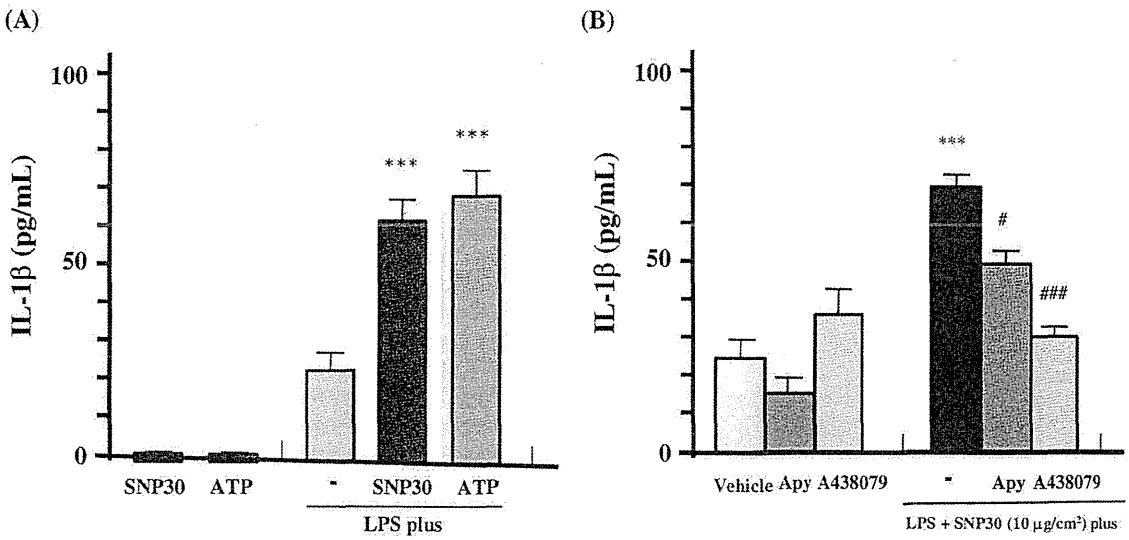

Fig. 4. ATP-induced IL-1β production and the inhibition of SNP30-induced IL-1β production by apyrase and A438079 in LPS-primed KUP5 cells. (A) ATP-induced IL-1β production. Cultivated KUP5 cells were stimulated with LPS (1 μg/mL) for 4 h, and then treated with ATP (1 mM) or SNP30 (10 μg/cm²) for 24 h. The culture supernatants were collected and the concentration of IL-1β was measured by means of enzyme-linked immunosorbent assay. Each value represents the mean ± S.E.M. of 4 independent assays. ***$P < 0.001$ vs. LSP-alone-treated group. (B) Inhibition of SNP30-induced IL-1β production by apyrase and $P2X_7$ antagonist A438079. Cultivated KUP5 cells were stimulated with LPS (1 μg/mL) for 4 h, then incubated with apyrase (5 U/mL) or A438079 (50 μM) for 30 min, followed by SNP30 (10 μg/cm²) for 24 h. The culture supernatants were collected and the concentration of IL-1β was measured by means of enzyme-linked immunosorbent assay. Each value represents the mean ± S.E.M. of 4 independent assays. ***$P < 0.001$ vs. Vehicle. #$P < 0.05$, ###$P < 0.001$ vs. (LPS plus SNP)-treated group.

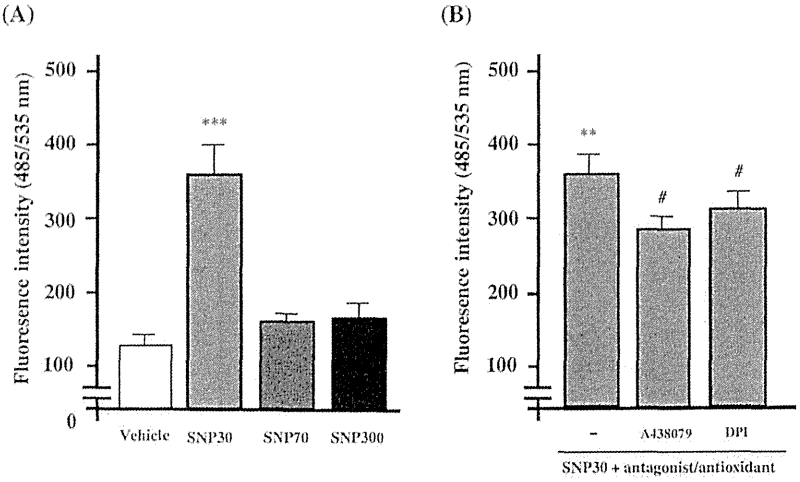

Fig. 5. ROS release induced by SNPs and inhibition of SNP30-induced ROS release by $P2X_7$ antagonist/ATP-release inhibitor A438079 and NADPH-oxidase inhibitor DPI in KUP5 cells. (A) ROS production by SNPs. KUP5 cells were treated with H_2DCF-DA (10 μM) for 30 min, and washed twice with DMEM. They were then stimulated with SNP30, SNP70 or SNP300 at a concentration of 10 μg/cm^2. Each value represents the mean ± S.E.M. of 8 independent assays. $^{***}P < 0.001$ vs. Vehicle. (B) Inhibition of SNP-induced ROS production by A438079 and DPI. The cells were first treated with H_2DCF-DA (10 μM) for 30 min, then washed twice with DMEM, and treated for 30 min with A438079 (50 μM) or DPI (100 μM) before exposure to SNP30 at a concentration of 10 μg/cm^2. DCF fluorescence was monitored for 10 min. $^{**}P < 0.01$ vs. Vehicle. $^{\#}P < 0.05$ vs. SNP30-treated group.

inhibited IL-1β production and significant suppression was also observed with Asc (1 mM), supporting the involvement of ROS in the cleavage of mature IL-1β.

4. Discussion

Activation of toll-like receptors (TLRs) by LPS triggers synthesis of inactive pro-IL-1β. This is cleaved to generate biologically active mature IL-1β by caspase-1, which is activated within large multi-protein complexes, termed inflammasomes. The NLRP3 and its adaptor protein apoptosis-associated speck-like protein (ASC), which are also components of inflammasomes, mediate caspase-1-dependent processing of pro-IL-1β (Agostini et al., (2004); Schroder and Tschopp, 2010). NLRP3 inflammasomes are activated by a variety of endogenous or exogenous stimuli such as ATP, monosodium urate (MSU) crystals, ROS, environmental pollutants silica and asbestos, and so-called danger signals including pathogen-associated molecular patterns (PAMPs) and danger-associated molecular patterns (DAMPs) (Agostini et al., 2004; Pétrilli et al., 2007; Schroder and Tschopp, 2010; Tschopp and Schroder, 2010). However, the mechanisms of activation of inflammasomes are not known in detail. Nevertheless, involvement of ROS seems to be common to all of the danger signals. In addition, it is known that extracellular ATP induces ROS production via cell-membrane NADPH oxidase via purinergic signaling (Noguchi et al., 2008; Ohshima et al., 2011; Suh et al., 2001; Uratsuji et al., 2012). Thus, it seems likely that both ATP and ROS participate in production of IL-1β through activation of inflammasomes via multiple signal transduction systems. Therefore, in this study, we looked in detail at the SNP-induced production of IL-1β in mouse Kupffer cell line KUP5, focusing on the roles of ATP release and purinergic signaling.

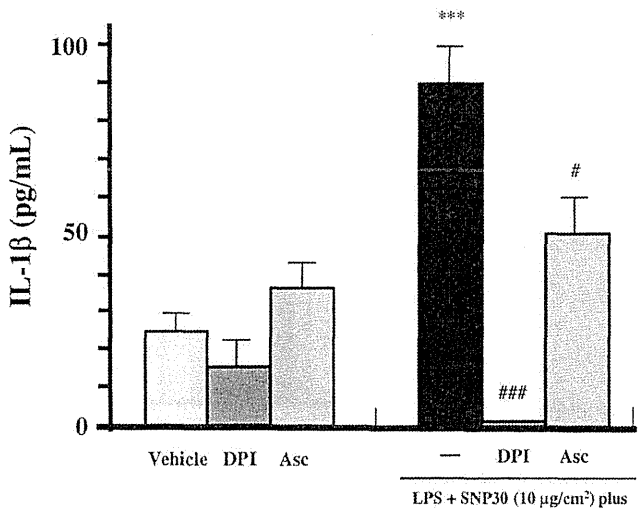

Fig. 6. Inhibition of NSP30-induced-IL-1β production by antioxidants. Effects of DPI and Asc on SNP30-induced IL-1β production. LPS-primed cells were pretreated with DPI (100 μM) or ascorbic acid (Asc, 1 mM) for 30 min before exposure to SNP30 at a concentration of 10 μg/cm^2. The cell culture supernatants were concentrated and IL-1β production was measured by enzyme-linked immunosorbent assay. $^{***}P < 0.001$ vs. Vehicle. $^{\#}P < 0.05$, $^{\#\#\#}P < 0.001$ vs. (LPS plus SNP30)-treated group.

First, we examined the relation between IL-1β production and ATP release in LPS-primed KUP5 cells. IL-1β production was increased in a dose-dependent manner by each of SNP30, SNP70, and SNP300. The dose-dependency of IL-1β production was also confirmed by the release of mature IL-1β from LPS-primed KUP5 cells exposed to SNP30 which was shown the greatest IL-1β production in these SNPs. The highest IL-1β production was observed at 24 h post-treatment with SNP30 at the dose of 10 μg/cm^2 or more. Similarly, ATP release was highest in the cells exposed to SNP30 at the dose of 10 μg/cm^2 or more. In addition, LPS-primed KUP5 cells treated with ATP alone showed almost the same level of IL-1β production as that treated with SNP30 alone. These results strongly suggest the involvement of extracellular ATP in IL-1β production by LPS-primed KUP5 cells. Next, to confirm the involvement of ATP, we examined the effects of the ecto-nucleotidase apyrase and the $P2X_7$ antagonist/ATP-release inhibitor A438079 on IL-1β production by LPS-primed KUP5 cells exposed to 10 μg/cm^2 SNP30. IL-1β production was significantly inhibited by both apyrase and A438079.

It has been reported that ATP is released from cells after various kinds of stimuli, including pH change, UV, ionizing radiation, osmotic pressure, and NPs, leading to a variety of receptor-mediated physiological effects. With regard to NPs, it has been reported that uric acid, silica, or alum particles induce release of intracellular ATP from human macrophages to the extracellular

space through $P2X_7$ receptor and connexin/pannexin channels (Riteau et al., 2012). We also showed that gamma-irradiation-induced ATP release depends on $P2X_7$ receptor, and further found that gap junction hemichannel connexin 43 is involved in radiation-induced ATP release in B16 melamona cells (Ohshima et al., 2012). Building on these findings, we examined ATP release from the LPS-primed KUP5 cells exposed to SNP in detail. Indeed, SNPs caused release of ATP, and the pattern of ATP release was consistent with that of IL-1β production.

ROS is well known to be involved in the activation of inflammasomes induced by danger signals, including PAMs and DAMPs. However, the precise mechanisms involved are still unknown. Here, we confirmed that exposure of LPS-primed KUP5 cells to SNP30 at the dose of 10 $\mu g/cm^2$ efficiently produced ROS, and the ROS production was inhibited by A438079 (a $P2X_7$ receptor antagonist) and DPI (an inhibitor of NADPH oxidase), supporting previous reports that extracellular ATP induces ROS formation via activation of cell-membrane NADPH oxidase through purinergic signaling mediated by activation of P2Y (Noguchi et al., 2008; Ohshima et al., 2011; Xia et al., 2006). These data suggest that ATP is released from $P2X_7$ receptor upon stimulation with NSP30, and degraded to ADP, leading to activation of P2Y receptor, followed by ROS production mediated by cell-membrane NADPH oxidase. However, a more detailed examination of the mechanisms underling SNP30-mediated NADPH oxidase activation is needed.

Although ROS appears to be commonly involved in triggering adverse effects induced by many kinds of nanoparticles (Manke et al., 2013; Xia et al., 2006), the signaling pathway(s) linking nucleotide release and ROS production have not been well studied (Dekali et al., 2012; Kobayashi et al., 2010; Palomäki et al., 2011; Xia et al., 2006). Meanwhile, it was reported that small latex beads (20 nm) induced the IL-1β production via ATP-$P2X_7$-dependent pathway, though IL-1β production by the latex beads was independent of ROS (Adachi et al., 2013). This result is contradictory to our present one. It is thought that this might be due to the cell type used or distinct surface properties of NPs.

In the present work, we have shown that ROS production in response to SNPs is at least partly mediated by purinergic signaling. This pathway may also contribute to ROS production stimulated by other kinds of NPs.

5. Conclusion

Our results indicate that stimulation of KUP5 cells with SNPs induces ATP release from $P2X_7$ receptor, leading to ROS production via membrane NADPH oxidase. The ROS activates inflammasomes, leading to production of mature IL-1β.

Conflict of interest

The authors declare that there are no conflicts of interest.

Transparency document

The Transparency document associated with this article can be found in the online version.

Acknowledgements

The authors thank Assistant Prof. Takeshi Kondo and graduate student Ms. Satomi Itoh for their assistance with dynamic light scattering (DLS) analysis of silica nanoparticles.This work was supported in part by a Grant-in Aid for Private University Science Research Upgrade Promotion, a Grant-in Aid for Health and Labor Sciences Research (Risk of Chemical Substances) from the Ministry of Health, Labor and Welfare, and a Grant-in Aid from the Foundation for Strategic Research at Private Universities, 2011–2015 (Grant No. S1101015).

References

Adachi, T., Takahara, K., Uchiyama, Y., Inaba, K., 2013. Particle size of latex beads dictates IL-1β production mechanism. PLoS ONE 8 (7), e68499.
Aillon, K., Xie, Y., El-Gendy, N., Berkland, C.J., Forrest, M.L., 2009. Effects of nano-material physicochemical properties on in vivo toxicity. Adv. Drug Deliv. Rev. 61, 457–466.
Agostini, L., Martinon, F., Burns, K., McDermott, M.F., Hawkins, P.N., Tschopp, J., 2004. NALP3 forms an IL-1β-processing inflammasome with increased activity in Muckle-Wells autoinflammatory disorder. Immunity 20, 319–325.
Bianchi, B.R., Lynch, K.J., Touma, E., Niforatos, W., Burgard, E.C., Alexander, K.M., Park, H.S., Yu, H., Metzger, R., Kowaluk, E., Jarvis, M.F., van Biesen, T., 1999. Pharmacological characterization of recombinant human and rat P2X receptor subtypes. Eur. J. Pharmacol. 376, 127–138.
Bodin, P., Burnstock, G., 2001. Purinergic signalling: ATP release. Neurochem. Res. 26, 959–969.
Borm, P.J., Kreyling, W., 2004. Toxicological hazards of inhaled manoparticles-potential implications for drug delivery. J. Nanosci. Nanotechnol. 4, 521–531.
Burnstock, G., 2007. Purine and pyrimidine receptors. Cell Mol. Life Sci. 64, 1471–1483.
Burnstock, G., 2014. Purinergic signalling: from discovery to current developments. Exp. Physiol. 99, 16–34.
Chen, Q., Xue, Y., Sun, J., 2013. Kupffer cell-mediated hepatic injury induced by silica nanoparticles in vitro and in vivo. Int. J. Nanomed. 8, 1129–1140.
Corriden, R., Insel, P.A., 2010. Basal release of ATP: an autocrine–paracrine mechanism for cell regulation. Sci. Signal. 3 (104), re1.
Crosera, M., Bovenzi, M., Maina, G., Adami, G., Zanette, C., Florio, C., Larese, F.F., 2009. Nanoparticle dermal absorption and toxicity: a review of the literature. Int. Arch. Occup. Environ. Health 82, 1043–1055.
Dekali, S., Divetain, A., Kortulewski, T., Vanbaelinghem, J., Gamez, C., Rogerieux, F., Lacroix, G., Rat, P., 2012. Cell cooperation and role of the P2X7 receptor in pulmonary inflammation induced by nanoparticles. Nanotoxicology 7, 1302–1314.
Deng, Z.J., Liang, M., Monteiro, M., Toth, I., Minchin, R.F., 2011. Nanoparticle-induced unfolding of fibrinogen promotes mac-1 receptor activation and inflammation. Nat. Nanotechnol. 6, 39–44.
Di Virgilio, F., Chiozzi, P., Falzoni, S., Ferrari, D., Sanz, J.M., Venketaraman, V., Baricordi, O.R., 1998. Cytolytic P2X purinoceptors. Cell Death Differ. 5, 191–199.
Donaldson, K., Tran, L., Jimenez, L.A., Duffin, R., Newby, D.E., Mills, N., MacNee, W., Vicki Stone, V., 2005. Combustion-derived nanoparticles: a review of their toxicology following inhalation exposure. Part. Fibre Toxicol. 2, 10, http://dx.doi.org/10.1186/1743-8977-2-10.
Feder, L.S., Todaro, J.A., Laskin, D.L., 1993. Characterization of interleukin-1 and interleukin-6 production by hepatic endothelial cells and macrophages. J. Leukoc. Biol. 53, 126–132.
Ferrai, D., Pizzirani, C., Adinolfi, E., Lemoli, R.M., Curti, A., Idzko, M., Panther, E., Di Virgilio, F., 2006. The P2X7 receptor: a key player in IL-1 processing and release. J. Immunol. 176, 3877–3883.
Franchi, L., Munoz-Planillo, R., Nunez, G., 2012. Sensing and reacting to microbes through the inflammasomes. Nat. Immunol. 13, 325–332.
Hasezaki, T., Isoda, K., Kondoh, M., Tsutsumi, Y., Yagi, K., 2011. Hepatotoxicity of silica nanoparticles with a diameter of 100 nm. Pharmazie 66, 698–703.
Humphreys, B.D., Dubyak, G.R., 1998. Modulation of P2X7 nucleotide receptor expression by pro- and anti-inflammatory stimuli in THP-1 monocytes. J. Leukoc. Biol. 64, 256–273.
Isoda, K., Tetsuka, E., Shimizu, Y., Saitoh, K., Ishida, I., Tezuka, M., 2013. Liver injury induced by thirty- and fifty-nanometer-diameter silica nanoparticles. Biol. Pharm. Bull. 36, 370–375.
Kitani, H., Takenouchi, T., Sato, M., Yoshioka, M., Yamanaka, N., 2011. A simple and efficient method to isolate macrophages from mixed primary cultures of adult liver cells. J. Vis. Exp. 51, 2757.
Kobayashi, T., Kouzaki, H., Kita, H., 2010. Human eosinophiles recognize endogenous ganger signal crystalline uric acid and produce proinflammatory cytokines mediated by autocrine ATP. J. Immunol. 184, 6350–6358.
Kolios, G., Valatas, V., Kouroumalis, E., 2006. Role of Kupffer cells in the pathogenesis of liver disease. World J. Gastroenterol. 12, 7413–7420.
Laskin, D.L., Pilaro, A.M., 1986. Potential role of activated macrophages in acetamino-phen toxicity. II. Mechanism of macrophage accumulation and activation. Toxicol. Appl. Pharmacol. 86, 216–226.
Laskin, D.L., Robertson, F.M., Pilaro, A.M., Laskin, J.D., 1988. Activation of liver macrophages following phenobarbital treatment of rats. Hepatology 8, 1051–1056.
Lazarowski, E.R., Sesma, J.I., Seminario-Vidal, L., Kreda, S.M., 2011. Molecular mechanisms of purine and pyrimidine nucleotide release. Adv. Pharmacol. 61, 221–261.
Lazarowski, E.R., Boucher, R.C., Harden, T.K., 2003. Mechanisms of release of nucleotides and integration of their action as P2X- and P2Y-receptor activating molecules. Mol. Pharmacol. 64, 785–795.
Liu, T., Li, L., Fu, C., Liu, H., Chen, D., Tang, F., 2012. Pathological mechanisms of liver injury caused by continuous intraperitoneal injection of silica nanoparticle. Biomaterials 33, 2399–2407.

Liu, C., Tao, Q., Sun, M., Wu, J.Z., Yang, W., Jian, P., Peng, J., Hu, Y., Liu, C., Liu, P., 2010. Kupffer cells are associated with apoptosis, inflammation and fibrotic effects in hepatic fibrosis in rats. Lab. Invest. 90, 1805–1816.
Luo, X., Morrin, A., Killard, A.J., Smyth, M.R., 2006. Application of nanoparticles in electrochemical sensors and biosensors. Electroanalysis 4, 319–326.
McCloskey, T.W., Todaro, J.A., Laskin, D.L., 1992. Lipopolysaccharide treatment of rats alters antigen expression and oxidative metabolism in hepatic macrophages and endothelial cells. Hepatology 16, 191–203.
Manke, A., Wang, L., Rojanasakul, Y., 2013. Mechanisms of nanoparticle-induced oxidative stress and toxicity. Biomed. Res. Int. 2013, 942916, http://dx.doi.org/10.1155/2013/942916.
Medina, C., Santos-Martinez, M.J., Radomski, A., Corrigan, O.I., Radomski, M.W., 2007. Nanoparticles: pharmacological and toxicological significance. Br. J. Pharmacol. 150, 552–558.
Michael, S.L., Pumford, N.R., Mayeux, P.R., Niesman, M.R., Hinson, J.A., 1999. Pretreatment of mice with macrophage inactivators decreases acetaminophen hepatotoxicity and the formation of reactive oxygen and nitrogen species. Hepatology 30, 186–195.
Morishige, T., Yoshioka, Y., Inakura, H., Tanabe, A., Yao, X., Narimatsu, S., Monobe, Y., Imazawa, T., Tsunoda, S., Tsutsumi, Y., Mukai, Y., Okada, N., Nakagawa, S., 2010. The effect of surface modification of amorphous silica particles on NLRP3 inflammasome mediated IL-1β production, ROS production and endosomal. Rupture Biomater. 31, 6833–6842.
Noguchi, T., Ishii, K., Fukutomi, H., Naguro, I., Matsuzawa, A., Takeda, K., Ichijo, H., 2008. Requirement of reactive oxygen species-dependent activation of ASK1-p38, MAPK pathway for extracellular ATP-induced apoptosis in macrophage. J. Biol. Chem. 283, 7657–7665.
Napierska, D., Thomassen, L.C.J., Lison, D., Martens, J.A., Hoet, P., 2010. The nanosilica hazard: another variable entity. Part. Fibre Toxicol. 7, 39.
Ohshima, Y., Kitami, A., Kawano, A., Tsukimoto, M., Kojima, S., 2011. Induction of extracellular ATP mediates increase in intracellular thioredoxin in RAW 264.7 cells exposed to low-dose γ-rays. Free Radic. Biol. Med. 51, 1240–1248.
Ohshima, Y., Tsukimoto, M., Takenouchi, T., Harada, H., Suzuki, A., Sato, M., Kitani, H., Kojima, S., 2010. Gamma-irradiation induces P2X(7) receptor-dependent ATP release from B16 melanoma cells. Biochim. Biophys. Acta 1800, 40–46.
Ohshima, Y., Tsukimoto, M., Harada, H., Kojima, S., 2012. Involvement of connexin 43 hemichannel in ATP release after γ-irradiation. J. Radiat. Res. 53, 551–557.
Palomäki, J., Välimäki, E., Sund, J., Vippola, M., Clausen, P.A., Jensen, K.A., Savolainen, K., Matikainen, S., Alenius, H., 2011. Long, needle-like carbon nanotubes and asbestos activate the NLRP3 inflammasome through a similar mechanism. ACS Nano 5, 6861–6870.
Pelegrin, P., Surprenant, A., 2006. Pannexin-1 mediates large pore formation and interleukin-1beta release by the ATP-gated P2X7 receptor. EMBO J. 25, 5071–5082.
Pilaro, A.M., Laskin, D.L., 1986. Accumulation of activated mononuclear phagocytes in the liver following lipopolysaccharide treatment of rats. J. Leukoc. Biol. 40, 29–41.
Pétrilli, V., Dostert, C., Muruve, D.A., Tschopp, J., 2007. The inflammasome: a danger sensing complex triggering innate immunity. Curr. Opin. Immunol. 19, 615–622.
Reisetter, A.C., Stebounova, L.V., Baltrusaitis, J., Powers, L., Gupta, A., Grassian, V.H., Monick, M.M., 2011. Induction of inflammasome-dependent pyroptosis by carbon black nanoparticles. J. Biol. Chem. 286, 21844–21852.
Riteau, N., Gasse, P., Fauconnier, L., Gombault, A., Couegnat, M., Fick, L., Kanellopoulos, J., Quesniaux, V.F., Marchand-Adam, S., Crestani, B., Ryffel, B., Couillin, I., 2010. Extracellular ATP is a danger signal activating P2X7 receptor in lung inflammation and fibrosis. Am. J. Respir. Crit. Care Med. 182, 774–783.
Riteau, N., Baron, L., Villeret, B., Guillou, N., Savigny, F., Ryffel, B., Rassendren, F., Le Bert, M., Gombault, A., Couillin, I., 2012. ATP release and purinergic signaling: a common pathway for particle-mediated inflammasome activation. Cell Death Dis. 3, e403.
Sandberg, W.J., Låg, M., Holme, J.A., Friede, B., Gualtieri, M., Kruszewski, M., Schwarze, P.E., Skuland, T., Refsnes, M., 2012. Comparison of non-crystalline silica nanoparticle in IL-1β release from macrophages. Part. Fibre Toxicol. 10 (9), 32, http://dx.doi.org/10.1186/1743-8977-9-32.
Schanen, B.C., Karakoti, A.S., Seal, S., Drake III, D.R., Warren, W.L., Self, W.T., 2009. Exposure to titanium dioxide nanomaterials provokes inflammation of an in vitro human immune construct. ACS Nano 3, 2523–2532.
Schroder, K., Tschopp, J., 2010. The inflammasomes. Cell 140, 821–832.
Suh, B.C., Kim, J.S., Namgung, U., Ha, H., Kim, K.T., 2001. P2X7 nucleotide receptor mediation of membrane pore formation and superoxide generation in human promyelocytes and neutrophils. J. Immunol. 166, 6754–6763.
Surprenant, A., Rassendren, F., Kawashima, E., North, R.A., Buell, G., 1996. The cytolytic P2Z receptor for extracellular ATP identified as a P2X receptor (P2X7). Science 272, 735–738.
Takenouchi, T., Ogihara, K., Sato, M., Kitani, H., 2005. Inhibitory effects of U73122 and U73343 on Ca^{2+} influx and pore formation induced by the activation of P2X7 nucleotide receptors in mouse microglial cell line. Biochim. Biophys. Acta 1726, 177–186.
Thakur, V., McMullen, M.R., Pritchard, M.T., Nagy, L.E., 2007. Regulation of macrophage activation in alcoholic liver disease. J. Gastroenterol. Hepatol. 22 (Suppl. 1), S53–S56.
Tschopp, J., Schroder, K., 2010. LRP3 inflammasome activation: the convergence of multiple signalling pathways on ROS production? Nat. Rev. Immunol. 10, 210–215.
Tsukimoto, M., Maehata, M., Harada, H., Ikari, A., Takagi, K., Degawa, M., 2006. P2X7 receptor-dependent cell death is modulated during murine T cell maturation and mediated by dual signaling pathways. J. Immunol. 177, 2842–2850.
Uratsuji, H., Tada, Y., Kawashima, T., Kamata, M., Hau, C., Asano, Y., Sugaya, M., Kadono, T., Asahina, A., Sato, S., Tamaki, K., 2012. P2Y6 Receptor signaling pathway mediates inflammatory responses induced by monosodium urate crystals gout occurs in individuals with hyperuricemia. J. Immunol. 188, 436–444.
Uskoković, V., 2013. Entering the era of nanoscience: time to be so small. J. Biomed. Nanotechnol. 9, 1441–1470.
Winter, M., Beer, H.D., Hornung, V., Kramer, U., Schins, R.P., Forster, I., 2011. Activation of the inflammasome by amorphous silica and TiO_2 nanoparticles in murine dendritic cells. Nanotoxicology 5, 326–340.
West, M.A., Billiar, T.R., Curran, R.D., Hyland, B.J., Simmons, R.L., 1989. Gastroenterology 96, 1572–1582.
Winwood, P.J., Arthur, M.J., 2006. Kupffer cells: their activation and role in animal models of liver injury and human liver disease. Semin. Liver Dis. 13, 50–59.
Xia, T., Kovochich, M., Brant, J., Hotze, M., Sempf, J., Oberley, T., Sioutas, C., Yeh, J.I., Wiesner, M.R., Nel, A.E., 2006. Comparison of the abilities of ambient and manufactured nanoparticles to induce cellular toxicity according to an oxidative stress paradigm. Nano Lett. 6, 1794–1807.
Yang, W., Peters, J.I., William III, R.O., 2008. Inhaled nanoparticles—a current review. Int. J. Pharm. 456, 239–247.
Yee, S.B., Ganey, P.E., Roth, R.A., 2003. The role of Kupffer cells and TNF-alpha in monocrotaline and bacterial lipopolysaccharide-induced liver injury. Toxicol. Sci. 71, 124–132.
Yazdi, A.S., Guarda, G., Riteau, N., Drexler, S.K., Tardivel, A., Couillin, I., Tschopp, J., 2010. Nanoparticles activate the NLR pyrin domain containing 3 (Nlrp3) inflammasome and cause pulmonary inflammation through release of IL-1α and IL-1β. Proc. Natl. Acad. Sci. U.S.A. 107, 19449–19454.
Yegutkin, G.G., 2008. Nucleotide- and nucleoside-converting ectoenzymes: Important modulators of purinergic signalling cascade. Biochim. Biophys. Acta 1783, 673–694.
Yu, Y., Li, Y., Wang, W., Jin, M., Du, Z., Li, Y., Duan, J., Yu, Y., Sun, Z., 2013. Acute toxicity of amorphous silica nanoparticles in intravenously exposed ICR mice. PLoS ONE 8, e61346, http://dx.doi.org/10.1371/journal.pone.0061346.
Zambetti, L.P., Laudisi, F., Licandro, G., Ricciardi-Castagnoli, P., Moretellaro, A., 2012. The rhapsody of NLRPs: master players of inflammation.. and a lot more. Immunol. Res. 53, 78–90.
Zhang, G., Zeng, X., Li, P., 2013. Nanomaterials in cancer-therapy drug delivery system. J. Biomed. Nanotechnol. 9, 741–750.

Toxicology 322 (2014) 61–68

Contents lists available at ScienceDirect

Toxicology

journal homepage: www.elsevier.com/locate/toxicol

Involvement of P2Y11 receptor in silica nanoparticles 30-induced IL-6 production by human keratinocytes

Chihiro Nagakura[a], Yusuke Negishi[a], Mitsutoshi Tsukimoto[a], Satomi Itou[b], Takeshi Kondo[b], Ken Takeda[c], Shuji Kojima[a,*]

[a] Department of Radiation Biosciences, Tokyo University of Science (TUS), 2641 Yamazaki, Noda-shi, Chiba 278-8510, Japan
[b] Research Institute for Science and Technology, Tokyo University of Science (TUS), 2641 Yamazaki, Noda-shi, Chiba 278-8510, Japan
[c] Department of Hygienic Chemistry, Faculty of Pharmaceutical Sciences, Tokyo University of Science (TUS), 2641 Yamazaki, Noda-shi, Chiba 278-8510, Japan

ARTICLE INFO

Article history:
Received 12 February 2014
Received in revised form 12 March 2014
Accepted 30 March 2014
Available online 2 May 2014

Keywords:
SNP30
IL-6 production
ATP
P2Y11 receptor
Skin inflammation

ABSTRACT

We have previously reported that P2Y11 receptor mediates IFN-γ-induced IL-6 production in human keratinocytes, suggesting the importance of purinergic signaling in skin inflammatory diseases. In this study, the involvement of various P2 receptors in IL-6 production induced by silica nanoparticle 30 (SNP30) was examined in a human keratinocyte cell line, HaCaT. Exposure to SNP30 increased IL-6 production in the cells. Ecto-nucleotidase (apyrase), a non-selective antagonist of P2Y receptors (suramin), and a selective P2Y11 receptor antagonist (NF157) all inhibited IL-6 production. Nucleotides such as ATP and UTP themselves also significantly increased IL-6 production in the cells. It was further confirmed that ATP was released from HaCaT cells exposed to SNP30. These results support the possible role of ATP in SNP30-induced IL-6 production by HaCaT cells.

In conclusion, these data demonstrate that P2Y11 receptor also mediates SNP30-induced IL-6 production in human keratinocytes, confirming that the ATP-P2Y11 purinergic signaling is a common pathway of IL-6 production leading to induction of skin inflammatory diseases.

1. Introduction

Various types of nanoparticles (NP) with novel electrical, catalytic, magnetic, mechanical, photonic and thermal properties have been developed and are already being used or tested in a wide range of consumer products, such as sunscreens, composites, and medical and electric devices. Specific properties of NP, such as their small size, shape, high surface area, and special structure, make these compounds promising candidates in both industries and biological applications (Luo et al., 2006; Uskoković, 2013; Yang et al., 2008; Zhang et al., 2013). However, in recent years, there has been increasing evidence of the adverse effects of NP (Aillon et al., 2009; Crosera et al., 2009; Donaldson et al., 2005; Medina et al., 2007; Xia et al., 2006). In the face of using NP, assessment of human health and environmental safety is now urgently required. On commercial available NP, such as silica, titanium oxide (TiO_2), silver, chrysotile asbestos, carbon nanotubes, and some magnetic particles, their biosafety and cytotoxicity have been now extensively investigated in vitro and in vivo experimental systems.

Silica NP (SNP), non-metal oxides, have been found extensive applications as additives such as cosmetics, medical supplies, the toner of the printer, the food, in various fields. Meanwhile, it is also concerned that a particle is uptaken by the living body in a process to use as a manufacturing process and a product, and unfavorable influence to the human body (Napierska et al., 2010).

The skin is composed of epidermis, dermis, and subcutaneous tissue, and serves to protect internal organs from potentially hazardous external factors, including mechanical stimuli, chemical stimuli, ultraviolet (UV) radiation, bacteria and so on. In the outer epidermal layer, about 95% of the cells are keratinocytes which produce various cytokines, such as interleukin-1 (IL-1), IL-6, IL-8, tumor necrosis factor-alpha (TNF-α), transforming growth factor-beta (TGF-β), platelet-derived growth factor, and chemokines (Ansel et al., 1990; Elder et al., 1989; Kock et al., 1990; Neuner et al., 1991; Schwarz and Luger, 1989). Production of these cytokines increases in response to environmental stimuli and injury (Kirnbauer et al., 1991; Kondo et al., 1993; Neuner et al., 1991).

IL-6, a well-studied inflammatory cytokine that plays a central role in immune responses, is produced by T cells, macrophages,

* Corresponding author. Tel.: +81 47121 3613; fax: +81 47121 3613.
E-mail address: kjma@rs.noda.tus.ac.jp (S. Kojima).

http://dx.doi.org/10.1016/j.tox.2014.03.010
0300-483X/

fibroblasts, keratinocytes, and endothelial cells. In keratinocytes, IL-6 induces proliferation and migration, thereby promoting skin repair (Bowman et al., 1997) and leading to skin diseases, such as psoriasis (Kawakami et al., 1997). UV is one of the hazardous external factors and produces IL-6 in the keratinocytes, resulting in thermal damage (Gallucci et al., 2004; Urbanski et al., 1990).

ATP is used as an energy source in cells, but extracellular ATP also acts as an intercellular signaling factor (Burnstock, 1997). Extracellular ATP is degraded to ADP, AMP, and adenosine by ecto-nucleotidases (Lazarowski et al., 2000). Purinergic receptors are receptors of these nucleotides, and are expressed on the membrane of cells. Activation of purinergic receptors induces various physiological effects (Dubyak and el-Moatassim, 1993). Purinergic receptors are categorized into adenosine receptor P1 receptors and ATP or ADP receptor P2 receptors. P2 receptors are classified into the ionotropic P2X1-7 receptor subtypes and the G-protein coupled P2Y1-14 receptor subtypes (Abbracchio and Burnstock, 1994). Purinergic receptors are expressed in human keratinocytes (Pastore et al., 2006), though the expression pattern of purinergic receptor subtypes depends on the grade of keratinocyte differentiation (Burrell et al., 2003; Dixon et al., 1999; Greig et al., 2003; Koegel and Alzheimer, 2001).

Cells, including keratinocytes, release ATP in response to various stimuli, such as mechanical stimuli, hypoosmotic stimuli, and radiation (Azorin et al., 2011; Koizumi et al., 2004; Mizumoto et al., 2003). The mechanisms of this release include a maxi-anion channel, P2X7 receptor/pore, a volume-sensitive outwardly rectifying chloride channel, a member of the ATP-binding cassette protein family, a gap junction hemichannel, and vesicular exocytosis (Fitz, 2007; Hisadome et al., 2002; Ohshima et al., 2010; Pankratov et al., 2006; Pellegatti et al., 2005; Sabirov et al., 2001; Sprague et al., 1998; Stout et al., 2002). ATP released from cells via these pathways activates P2 receptors in an autocrine or a paracrine manner (Corriden and Insel, 2010). Recently, it has been found that extracellular ATP induces IL-6 production via P2Y receptors (Inoue et al., 2007; Ishimaru et al., 2013; Yoshida et al., 2006). Moreover, it has already been reported that SNP produces IL-6 by keratinocytes under UV exposure, but not in the dark condition (Koizumi et al., 2004). However, the mechanism of cytokine-induced IL-6 production by keratinocytes is not fully understood. In this study, we investigated the involvement of extracellular ATP and various P2 receptors in IL-6 production induced by 30-nanometer silica nanoparticle (SNP30) in a human keratinocyte cell line, HaCaT.

2. Materials and methods

2.1. Reagents

SNP of diameters with 30, 70, and 300 nm (designated as SNP30, SNP70 and SNP300) were purchased from Micromod Partikeltechnologie GmbH). Dulbecco's modified Eagle's medium containing 1.0 g glucose/L (low-glucose type DMEM), 100U/mL penicillin, 0.1 mg/mL streptomycin, dithiothreitol (DTT), polyoxyethylene sorbitan monolaurate (equivalent of Tween-20), and 10%FBS were purchased from Wako Pure Chemical Industries (Osaka, Japan). ATP, UTP, and apyrase were from Sigma–Aldrich (St. Louis, MO). Fetal bovine serum (FBS) was from Biowest (Nuaillé, France). The broad-spectrum P2X antagonist pyridoxal phosphate-6-azo (benzene-2,4-disulfonic acid) tetrasodium salt hydrate (PPADS), the P2Y12 antagonist clopidogrel and the broad-spectrum P2Y antagonist suramin sodium salt (suramin) were obtained from Sigma–Aldrich (St. Louis, MO). The P2X7 antagonist N-[2-[[2-[(2-hydroxyethyl)-amino]ethyl]amino]-5-quinolinyl]-2-tricyclo-[3.3.1.13,7]-dec-1-ylacetamide dihydro-chloride (AZ10606120), the P2Y1 antagonist 2′-deoxy-N-6-methyl-adenosine 3′,5′-bisphosphate tetrasodium salt (MRS2179), the P2Y6 antagonist N,N″-1,4-butanediylbis[N′-(3-isothiocyanatophenyl)thiourea (MRS2578), the P2Y13 antagonist 2-[(2-chloro-5-nitrophenyl)azo]-5-h ydroxy-6-methyl-3-[(phosphonooxy)-methyl]-4-pyridine carboxaldehyde disodium salt (MRS2211), and the P2Y11 antagonist 8,8′-[carbonylbis[imino-3,1-phenylene carbonylimino (4-fluoro-3,1-phenylene) carbonyl-imino]] bis-1,3,5-naphthalenetrisulfonic acid hexasodium salt (NF157) were from Tocris Bioscience (Ellisville, MO). All other chemicals used were of the highest purity available.

2.2. Characterization of silica NPs

The particle size distribution of SNP30, SNP70, and SNP300 in DMEM was evaluated by dynamic light-scattering (DLS), using NICOMP 370 (Particle Sizing System, Co., Tokyo Japan). Briefly, 2.5 mg of each SNP was suspended in 1 mL low-glucose type DMEM, mixed thoroughly with vortex mixture, and immediately subjected to DLS analysis at room temperature. Morphology of SNP30 prepared by the same method was assessed at room temperature by transmission electron microscopy (TEM), using a JEOL JEM 2010 (JEOL Ltd., Tokyo, Japan). SNP30 suspended in low-glucose type DMEM was dropped on the 400 mesh grid coated with carbon membrane, kept for 2 h at 37 °C, and then dried. The dried SNP30 was observed by TEM.

2.3. Reverse transcription polymerase chain reaction (RT-PCR)

Total RNA was isolated from HaCaT cells using a Relia Pre™ RNA cell Minipre System kit (Promega Co., WI). The first-strand cDNA was synthesized from total RNA with PrimeScript Reverse Transcriptase (Takara Bio). Specific primers were designed with PrimerQuest ™ (Integrated DNA Technologies, Inc., Coralville, IA) and synthesized by Sigma Genosys. The sequences of specific primers used in this study are shown in Table 1. GAPDH mRNA was determined as a positive control. PCR was carried out by incubating each cDNA sample with the primers (0.5 M each), PrimeSTAR HS DNA Polymerase (1.25 units, Takara Bio), and a deoxynucleotide mixture (0.2 mM each, Takara Bio). After the samples were incubated at 95 °C for 2 min, amplification was carried out for 35 cycles (each cycle: 95 °C for 30 s, annealing at 65 °C for 1 min and incubated at 72 °C for 10 min. The products were then subjected to 2% agarose gel electrophoresis. Bands were stained with ethidium bromide and photographed.

2.4. Assay of extracellular ATP

Cells were exposed to SNP30 and the extracellular ATP concentration was measured using ENLITEN rLuciferase/Luciferin Reagent (Promega, Madison, WI). At the indicated time points, each sample was centrifuged at 600 × g for 1 min and 10 μL of the supernatant was collected for ATP determination. The concentration of ATP was determined by measuring chemiluminescence with a Wallac 1420 ARVO fluoroscan (Wallac, Turku, Finland) after adding 100 μL of luciferin-luciferase reagent to 10 μL of sample solution.

2.5. Assay of IL-6, TNF-α, and IFN-γ

HaCat cells were stimulated with SNPs and incubated. The culture supernatants were collected and measured the concentrations of IL-6 and TNF-α by enzyme-linked immunosorbent assay as mentioned below. The cells were exposed to various doses of SNP30 for 24 h. The culture supernatants were collected and the concentration of TNF-α was measured by enzyme-linked immunosorbent assay. In another experiment, the cells were pre-incubated with apyrase (5 U/mL) for 10 min, and PPADS (100 μM), AZ10606120 (10 μM), suramin (100 μM), MRS2179 (100 μM), MRS2578 (10 μM), NF157 (50 μM), clopidogrel (30 μM), or MRS2211 (100 μM) for 30 min, and further incubated for 24 h, and the concentration of IL-6 in supernatants was assayed. A 96-well plate was coated with purified anti-human IL-6 or TNF-α mAb (1:500) (eBioscience) and incubated overnight at 4 °C. The plate was washed with PBS containing 0.05% Tween 20. Phosphate-buffered saline containing 1% BSA was added to the plate and the plate was incubated at room temperature to block the non-specific binding. The plated was washed, and added the supernatants were added for 2 h at room temperature. After washing, biotin-conjugated anti-human IL-6 mAb (1:1000) or TNF-α mAb (1:500) (eBioscience) was added for 1 h room temperature. The plate was washed, and added avidin-horseradish peroxidase (Sigma) for 30 min at room temperature. The plate was further washed, and added 3,3′,5,5′-tetramethylbenzidine for a few minutes to stain. The reaction was stopped by adding 2.5 M H_2SO_4. The absorbance at 450 nm was measured with a Wallac 1420 ARVO fluoroscan (Wallac, Turku, Finland). The concentration of IFN-γ was measured using Quantikine ELISA kit for human IFN-γ (R&D Systems, Inc., MN, USA) following manufacturer's instructions. A standard curve was established with recombinant human IL-6 (15.6–1000 pg/mL), IFN-γ (15.6–1000 pg/mL) or TNF-α (15.6–1000 pg/mL) (eBioscience), and the concentration of IL-6 or TNF-α was estimated from the standard curve.

2.6. Cell viability

A colorimetric assay with WST-1 reagent was used to evaluate cell viability in accordance with the manufacturer's directions. HaCaT cells (1×10^5/mL) were exposed to 5 μg/cm² of SNP30 for 24 h. Then 10 μL of WST-1 reagent, diluted 4-fold in phosphate buffer, was added to each well and incubation was continued for another 4 h at 37 °C. The absorbance of the wells at 450 nm was measured with a plate reader. Relative cell viability was calculated as a percentage of the control group, to which SNP30 had not been added.

Table 1
Primers of P2 receptors.

Gene	Primers (forward and reverse)	Accession number in GenBank	Product size (bp)
P2X1	5′-CCAGCTTGGCTACGTGGTGCAAGA-3′ 5′-ACGGTAGTTGGTCCCGTTCTCCACAA-3′	U45448	226
P2X2	5′-CCCGAGAGCATAAGGGTCCACAAC-3′ 5′-AATTTGGGGCCATCGTACCCAGAA-3′	AF190823	208
P2X3	5′-CCCCTCTTCAACTTTGAGAAGGGA-3′ 5′-GTGAAGGAGTATTTGGGGATGCAC-3′	NM002559	245
P2X4	5′-CCTTCCCAACATCACCACTACTTACC-3′ 5′-AGGAGATACGTTGTGCTCAACGTC-3′	U85975	256
P2X5	5′-AGCACGTGAATTGCCTCTGCTTAC-3′ 5′-ATCAGACGTGGAGGTCACTTTGCTC-3′	AF016709	183
P2X6	5′-GGTTTCCGTCACTCAGATCAAGG-3′ 5′-GGCACCAACTCCAGATCTCAC-3′	AF065385	290
P2X7	5′-CTGCTCTCTTGAACAGTGCCGAAA-3′ 5′-AGTGATGGAACCAACGGTCTAGGT-3′	Y09561	270
P2Y1	5′-ACCTCAGACGAGTACCTGCGAAGT-3′ 5′-AGAATGGGGTCCACACAACTGTTGAG-3′	NM002563	353
P2Y2	5′-GTGTCTGGGCGTCTTACGACCTCT-3′ 5′-AGAATGGGGTCCACACAACTGTTGAG-3′	NM176072	215
P2Y4	5′-GTGTCCTTTTCCTCACCTGCATCA-3′ 5′-ACGAGCCATGAGTCCATAGCAAAC-3′	NM002565	311
P2P6	5′-TTCAGGCTGAGGAGATGGGT-3′ 5′-GCCAGAGCAAGGTTTAGGGT-3′	HSU52464	286
P2Y11	5′-AGAAGCTGCGTGTGGCAGCGTTGGT-3′ 5′-ACGGTTTAGGGGCGGCTGTGGCATT-3′	AY449733	369
P2Y12	5′-GGAACAGGACCACTGAGAAC-3′ 5′-TCATGCCAGACTAGACCGAA-3′	AF313449	302
P2Y13	5′-CCTTTCAAAATCCTCTCTGACTC-3′ 5′-TCCTTGTTGCTCAAGATCGT-3′	NM023914	266
P2Y14	5′-CTCTGCCGTGCTCTTCTACGTCAA-3′ 5′-TTAATGCTTTGTGCCACTTCCGT-3′	NM014879	275
GAPDH	5′-GAAGGTGAAGGTCGGAGTC-3′ 5′-GAAGATGGTGATGGGATTTC-3′	NM002046	242

2.7. Statistics

Results are expressed as the mean ± S.E.M. The statistical significance of differences between two groups was calculated by using the unpaired Student's *t*-test. The statistical significance of differences between control and other groups was calculated by using Dunnett's test. The criterion of significance was $P < 0.05$ as determined with the Instat version 3.0 statistical package (Graph Pad Software, San Diego, CA).

3. Results

3.1. Characterization of SNPs

Since NPs often agglomerates in culture medium, the average sizes of SNP30, SNP70, and SNP300, suspended in low-glucose type DMEM, were analyzed by DSL. Furthermore, the form of SNP30 in the low-glucose type DMEM were observed by TEM. As shown in Fig. 1A–C, the average particle diameters of SNP30, SNP70 and SNP300 were 35.1, 65.6 and 278.7 nm, respectively, in the medium. TEM micrographs revealed that the majority of SNP30 had the primary particle size of less than <50 nm and were approximately uniformly dispersed in the medium (Fig. 1D).

3.2. Dose- and time-dependent effects of SNP30 on IL-6 production by HaCaT cells

Dose- and time-dependent effects of SNP30 on IL-6 production in HaCaT cells was examined. As shown in Fig. 2B, IL-6 was increased from doses of 5 μg/cm^2 up to 50 μg/cm^2, in a dose dependent manner. As shown in Fig. 2B, IL-6 production was increased in a time-dependent manner up to 24 h in the cells exposed to SNP30. It is noted that the viability of SNP30-exposed cells were not reduced at 24 h post-treatment by means of WST-1 assay (data not shown) in comparison with the control group. These results suggest that SNP-30 induces IL-6 production by HaCaT cells.

In the following experiments, assay of IL-6 was fixed the time at 24 h after the exposure to 5 μg/cm^2 of SNP.

3.3. Size-dependent effect of SNPs on IL-6 production in HaCat cells

Effect of three different sizes of SNPs, including SNP30, SNP70 and SNP300, on IL-6 production by HaCaT cells was examined at a fixed dose of 5 μg/cm^2. As shown in Fig. 3, among these SNPs with different sizes, SNP30 efficiently produced IL-6 at 24 h after the exposure.

3.4. Effects of SNP30 on production of TNF-α and INF-γ by HaCaT cells

Since TNF-α and IFN-γ are important modulators in immune responses, the production was also examined at different doses of SNP30. As shown in Fig. 4, the productivity by HaCaT cells was significantly low at 24 h after SNP30 exposure, and significant changes were not observed at any doses. As to IFN-γ, the level of IFN-γ released from HaCaT cells exposed to SNP30 was very low, and could not be detected.

3.5. Involvement of P2 receptors in SNP-induced IL-6 production by HaCaT cells

First, the expression of P2Y11 receptor in HaCaT cells was confirmed by RT-PCR. The cells strongly expressed P2Y11 together with P2X2, 4, 5 and P2Y1, 2, 6 receptor subtypes (Fig. 5A). Receptors of P2X7 and P2Y4, 12, 14 were shown some expression. Next, effect of ecto-nucleotidase apyrase and non-specific/specific P2 receptor antagonists on IL-6 production were examined in order to investigate whether P2 receptors are involved in SNP30-induced IL-6 production. The sample in the absence of SNP30

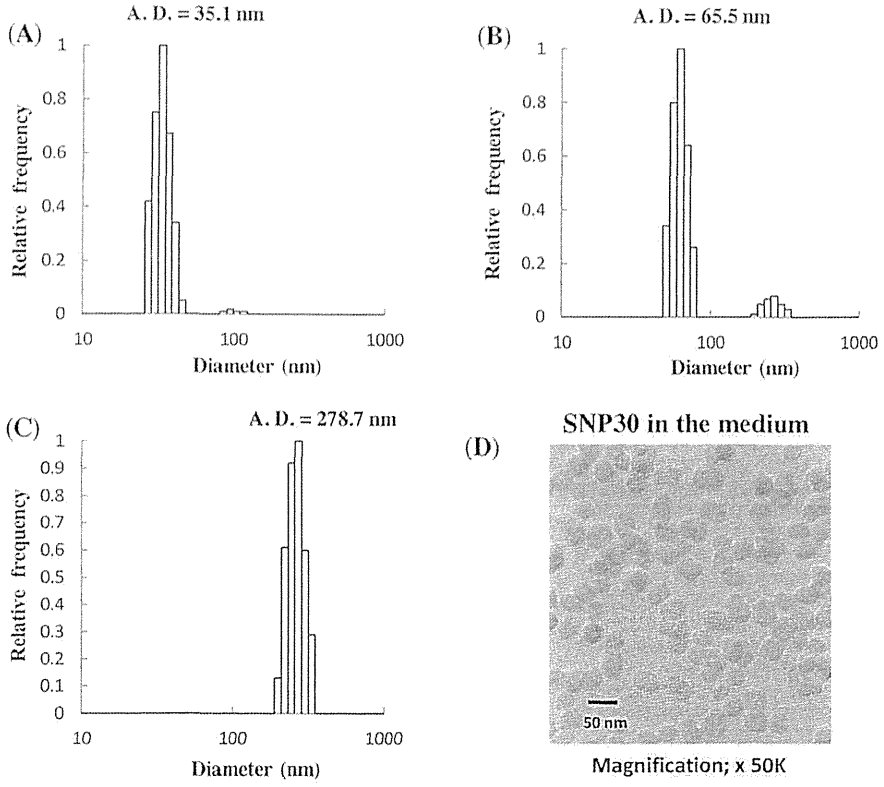

Fig. 1. Distribution of SNP30, SNP70, and SNP300 in DMEM by dynamic light-scattering (DLS) and morphology of SNP30 in PBS by transmission electron microscopy (TEM). (A)–(C) Distribution of SNP30, SNP70, and SNP300 by DLS, respectively. (D) Micrograph of SNP 30 in DMEM by TEM. A.D., average particle diameter. Scale bar, 100 nm.

(vehicle) was measured as a control. IL-6 production was significantly decreased by pre-treatment with apyrase, a broad antagonist of P2X receptor PPADS and a non-specific antagonist of P2Y receptors (suramin), and the P2Y11 receptor-specific antagonist NF157 (Fig. 5B), suggesting that P2Y11 receptor is involved in SNP30-induced IL-6 production in HaCaT cells. Whereas antagonists of the P2Y12 receptor- and the P2Y13 specific-receptor, clopidogrel and MRS2211, respectively, significantly increased IL-6 production. These data may suggest that both receptors were involved in the suppression of IL-6 production.

3.6. Induction of IL-6 production by P2 receptor agonists and their blockage by antagonists

P2 receptor agonist-induced IL-6 production and its blockage by suramin and NF157 were examined in HaCaT cells. As shown in Fig. 6, agonists, such as ATP and UTP, significantly increased IL-6 production by HaCaT cells at 24 h after the treatments. These increases induced by ATP and UTP were significantly blocked by suramin. Furthermore, the P2Y11 receptor-specific antagonist NF157 further reduced IL-6 production.

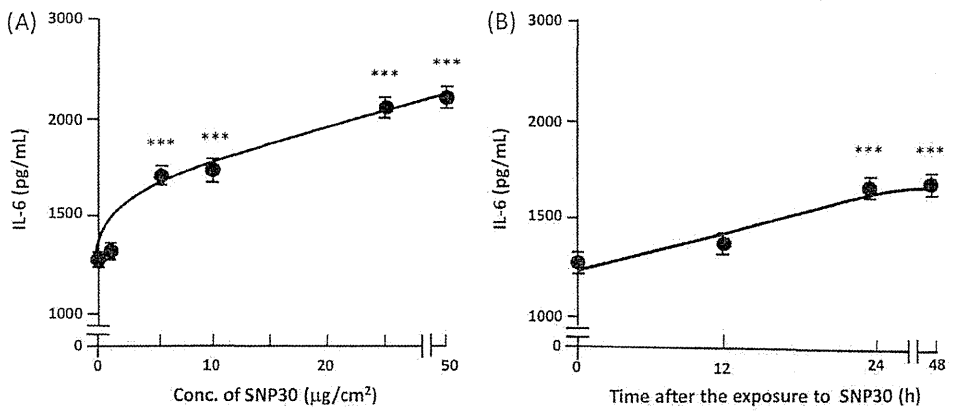

Fig. 2. Dose- and time-dependent effects of SNP30 on IL-6 production by HaCaT cells. (A) Dose-dependent effect of SNP30 on IL-6 production by the cells. HaCaT cells (1×10^5/mL) were exposed to SNP30 for 24 h at various doses from 1 to 50 μg/cm². The culture supernatants were collected and the concentration of IL-6 was measured by enzyme-linked immunosorbent assay. Each value represents the mean ± S.E.M. of four independent assays. ***$P < 0.001$ vs. the SNP conc. 0 (μg/cm²) group. (B) Time-dependent effect of SNP30 on IL-6 production by the cells. HaCaT cells were exposed to SNP30 at a fixed dose of 5 μg/cm² for the indicated time. The culture supernatants were collected at each time and the concentration of IL-6 was measured by enzyme-linked immunosorbent assay. Each point represents the mean ± S.E.M. of four independent assays. ***$P < 0.001$ vs. the time 0 h point.

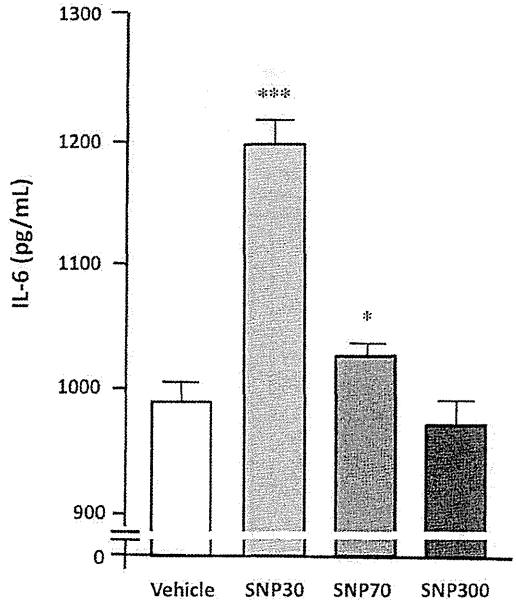

Fig. 3. Size-dependent effect of SNP30, SNP70, and SNP300 on IL-6 production by HaCaT cells. HaCaT cells were exposed to SNPs for 24 h at a dose of 5 μg/cm². After incubation, IL-6 in the culture medium was measured by enzyme-linked immunosorbent assay. Each value represents the mean ± S.E.M. of four independent assays. *$P < 0.05$, ***$P < 0.001$ vs. Vehicle group.

3.7. *Effect of SNP30 exposure on extracellular ATP release and its comparison with SNPs with a different size*

The time-dependent effect of SNP30 on ATP release from HaCaT cells was examined at the fixed dose of 5 μg/cm². As shown in Fig. 7A, the release was significantly increased between 40 and 50 min post-treatment, and followed by returning to the control level. Then, the ATP release was examined among these three SNPs, SNP30, SNP70 and SNP300, at 40 min post-treatment. As shown in Fig. 7B, significant ATP release was obtained in SNP30, and the moderate release was in SNP70. The release by SNP300 was almost similar to the SNP-non-treated control.

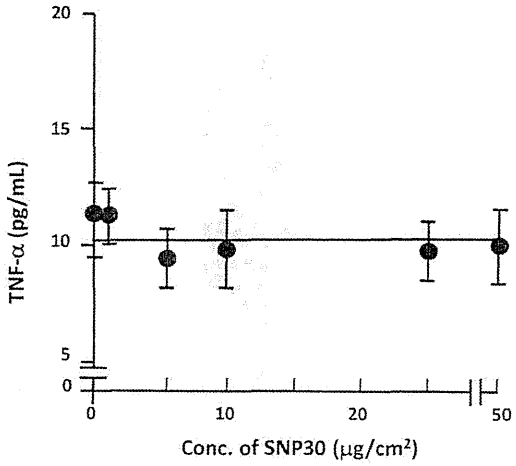

Fig. 4. Dose-dependent effects of SNP30 on TNF-α production by HaCaT cells. HaCaT cells were exposed to various doses of SNP30 for 24 h. The culture supernatants were collected and the concentration of TNF-α was measured by enzyme-linked immunosorbent assay. Each value represents the mean ± S.E.M. of four independent assays.

4. Discussion

Though it has been well known that metal-based nanoparticles produce IL-6 production in skin keratinocytes (Manke et al., 2007), there are only a few reports concerning SNP-induced IL-6 production in the keratinocytes; SNP produces IL-6 under UVB exposure in HaCaT cells (Wilkin et al., 2001). As to the mechanism, it is suggested that SNP generates radical oxygen species, leading to triggering the proinflammatory cytokines such as IL-1, IL-6, and TNF-α. First of all, whether SNP induces IL-6 production human keratinocyte cell line, HaCaT. The production of IL-6 was increased in HaCaT cells exposed to SNP30. The increase was markedly suppressed by a P2X broad antagonist, a non-selective P2Y receptor antagonist and a P2Y11 receptor-selective antagonist, while other P2 receptor selective antagonists had no effect. These results suggest that P2Y11 receptor is mainly involved in SNP30-induced IL-6 production.

It has already been shown that extracellular ATP induces IL-6 production in human keratinocytes (Inoue et al., 2007; Yoshida et al., 2006). Then, involvement of extracellular ATP and P2 receptors in IL-6 production was examined. As a result, ATP itself markedly increased IL-6 production by HaCaT cells at 24 h after the treatment. Besides, another agonist UTP, also significantly increased the production. These increased production were significantly blocked by suramin and NF157, strongly supporting involvements of extracellular ATP and P2Y11 receptor in IL-6 production by HaCaT cells. Then effect of ecto-nucleotidase apyrase on SNP30-induced IL-6 production was examined. Pre-treatment with apyrase significantly inhibited IL-6 production, supporting that extracellular ATP activates P2Y11 receptor and induces IL-6 production.

Finally, release of ATP from the HaCaT cells exposed to SNP30 was examined. It was found that the released ATP into the culture medium from the cells was significantly increased by exposure to SNP30 during the times between 40 and 50 min after SNP30 treatment, indicating that HaCaT cells exposed to SNP30 release ATP. Comparing with the extent of ATP release among SNPs with a different size, the release from the cells exposed to SNP30 at 40 min post-treatment was much higher than those of SNP70 and SNP300. These results were well accorded with those of production of IL-6 by HaCaT cells.

It has been well established that ATP releases from keratinocytes in response to mechanical stimuli (Corriden and Insel, 2010). As for the pathway of ATP release from HaCaT cells exposed to SNP30, our previous report indicated that IFN-γ-induced IL-6 production was reduced by anion transporter blocker FFA, cystic fibrosis transmembrane conductance regulator blocker glibenclamide, and maxi-anion channel blocker $GdCl_3$, indicating that anion channels are involved in the ATP release. It has already been reported that HaCaT cells irradiated with γ-rays also release ATP via a similar pathway (Tsukimoto et al., 2010). Thus, anion channels may be the key pathway of ATP release in response to various external stimuli in HaCaT cells. Thus, it is thought that SNP30 also induces ATP release and physiological action in the same ways, not experimenting in this study.

Recent studies have shown that P2Y receptors play an important role in cellular responses. For examples, this receptor mediates the anti-apoptotic effect of ATP in human neutrophils (Manke et al., 2007). Nucleotides induce cytokine release via P2Y11 receptor in human monocyte-derived dendritic cells (Wilkin et al., 2001). In bile duct epithelia, extracellular ATP enhances IL-6 production via P2Y11 receptor (Bingle et al., 2007). Other subtypes of purinergic receptors also have important functions; Monosodium urate crystal produced IL-6 via P2Y6 receptor signaling pathways (Boudreault and Grygorczyk, 2004; Uratsuji et al., 2012).

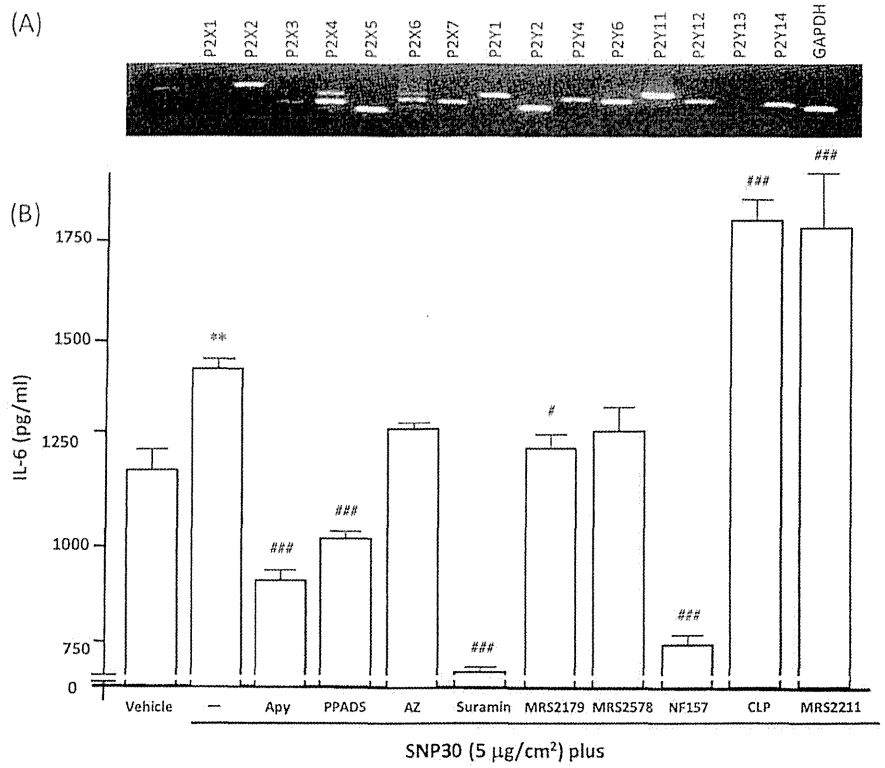

Fig. 5. Involvement of P2 receptors in SNP30-induced IL-6 in HaCaT cells. (A) The expression of P2 receptor subtypes in HaCaTcells. Total RNA was extracted from HaCaT cells, and the expression of P2 receptors mRNA in these cells was analyzed by RT-PCR. GAPDH mRNA was determined as a positive control. (B) The effect of ecto-nucleotidase and P2 receptor antagonists on SNP-induced IL-6 production. HaCaT cells were pre-incubated with apyrase (Apy., 5 U/mL) for 10 min, and PPADS (100 μM), AZ10606120 (10 μM), suramin (100 μM), MRS2179 (100 μM), MRS2578 (10 μM), NF157 (50 μM), clopidogrel (30 μM), or MRS2211 (100 μM) for 30 min. At 24 h after the expoposure to SNP30 (5 μg/cm²), the concentration of IL-6 in supernatants was measured by ELISA. Each value represents the mean ± S.E.M. of four independent assays. $^{**}P < 0.01$ vs. Vehicle group. $^{\#}P < 0.05$, $^{\#\#\#}P < 0.001$ vs. SNP30 alone-treated group.

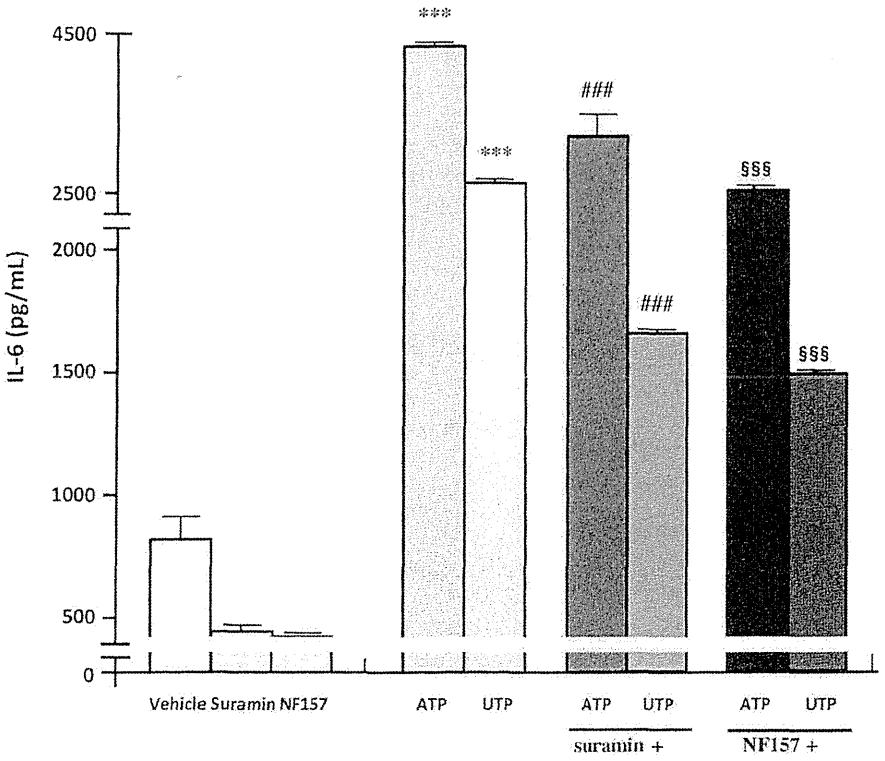

Fig. 6. Effect of P2 receptor agonists on IL-6 production and their inhibition by P2Y antagonist suramin in HaCaT cells. HaCaT cells were incubated with agonists such as ATP and UTP instead of SNP30 for 24 h and the concentration of IL-6 in supernatants was assayed. In another experiment, the cells were pre-incubated with P2Y antagonist suramin (100 μM) or NF157 (50 μM) for 30 min and further incubated with ATP or UTP for 24 h, and the concentration of IL-6 in supernatants was assayed. Each value represents the mean ± S.E.M. of four independent assays. $^{***}P < 0.001$ vs. Vehicle group. $^{\#\#\#}P < 0.001$ vs. ATP alone-treated group. $^{\S\S\S}P < 0.001$ vs. UTP alone-treated group.

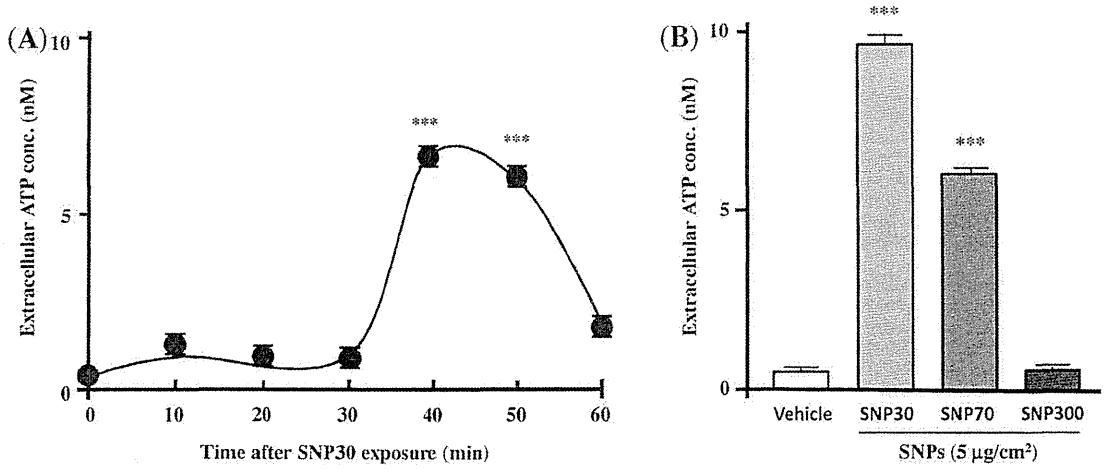

Fig. 7. ATP release from HaCaT cells exposed to SNP30 and its comparison among. SNP30, SNP70 and SNP300. (A) Time-dependent effect of SNP30 on ATP release from HaCaT cells. The cells were exposed to SNP30 for the indicated times. After incubation, the concentration of ATP in the culture medium was measured by luciferin/luciferase assay. Each value represents the mean ± S.E.M of four independent assays. ***$P < 0.01$ vs. the time 0 min. (B) Comparison of ATP release from HaCaT cells among SNP30, SNP70 and SNP300. The cells were exposed to each SNP at a dose of 5 μg/cm² for 40 min. After incubation, the concentration of ATP in the culture medium was measured by luciferin/luciferase assay. Each value represents the mean ± S.E.M of four independent assays. ***$P < 0.01$ vs. Vehicle group.

There are many kinds of cytokines, among which pro-inflammatory cytokines, such as IL-1β, IL-6, TNF-α, IFN-γ, IL-8, are essential for immune functions. Namely, IL-1α, IL-1β, and TNF-α enhance the synthesis of IL-6 (Kirnbauer et al., 1989; Partridge et al., 1991). IL-6 induces cell proliferation and migration, playing a physiological role in wound repair (Lazarowski et al., 2000). Besides, IFN-γ is a factor required for IL-6 production in keratinocytes (Farrar and Schreiber, 1993; Gröne, 2002). We also assayed IFN-γ in this study. However, the level of IFN-γ released from HaCaT cells exposed to SNP30 was very low, and could not be detected. These results would suggest that the production of IL-6 will be induced through other IFN-γ-independent signaling pathways. Furthermore, it is already revealed that ATP induces these pro-inflammatory cytokines in immune cells such as macrophages (Ferrari et al., 1997). Thereby, such an indirect action of IFN-γ via ATP release will enhance the level of pro-inflammatory cytokines, resulting in a synergistic IL-6 production in various cells including keratinocytes. Study of SNP30-induced IL-6 production associated with these cytokines is now underway.

In conclusion, it would be suggested SNP30 induces IL-6 production via ATP signaling in HaCaT cells through P2Y11 receptor.

Conflict of interest

The authors declare that there are no conflicts of interest.

Transparency document

The Transparency document associated with this article can be found in the online version.

Acknowledgements

This work was in part supported by a Grant-in Aid for the Private University Science Research Upgrade Promotion Business "Academic Frontier Project, a Grants-in Aid for Health and Labor Sciences Research Grants, Research Risk of Chemical Substances, from the Ministry of Health, Labor and Welfare" and a Grant-in Aid for NEXT-Supported Program for the Strategic Research Foundation at Private Universities, 2011–2015.

References

Abbracchio, M.P., Burnstock, G., 1994. Purinoceptors: are there families of P2X and P2Y purinoceptors? Pharmacol. Ther. 64, 445–475.
Aillon, K., Xie, Y., El-Gendy, N., Berkland, C.J., Forrest, M.L., 2009. Effects of nano-material physicochemical properties on in vivo toxicity. Adv. Drug 61 (6), 457–466.
Ansel, J., Perry, P., Brown, J., Damm, D., Phan, T., Hart, C., Luger, T., Hefeneider, S., 1990. Cytokine modulation of keratinocyte cytokines. J. Invest. Dermatol. 94, 101S–107S.
Azorin, N., Raoux, M., Rodat-Despoix, L., Merrot, T., Delmas, P., Crest, M., 2011. ATP signalling is crucial for the response of human keratinocytes to mechanical stimulation by hypo-osmotic shock. Exp. Dermatol. 20, 401–407.
Bingle, C.D., Sabroe, I., Surprenant, A., Whyte, M.K., 2007. Inhibition of neutrophil apoptosis by ATP is mediated by the P2Y11 receptor. J. Immunol. 179, 8544–8553.
Boudreault, F., Grygorczyk, R., 2004. Cell swelling-induced ATP release is tightly dependent on intracellular calcium elevations. J. Physiol. 561, 499–513.
Bowman, P.D., Schuschereba, S.T., Lawlor, D.F., Gilligan, G.R., Mata, J.R., DeBaere, D.R., 1997. Survival of human epidermal keratinocytes after short duration high temperature: synthesis of HSP70 and IL-8. Am. J. Physiol. 272, C1988–C1994.
Burnstock, G., 1997. The past, present and future of purine nucleotides as signalling molecules. Neuropharmacology 36, 1127–1139.
Burrell, H.E., Bowler, B., Gallagher, J.A., Sharpe, G.R., 2003. Human keratinocytes express multiple P2Y-receptors: evidence for functional P2Y1, P2Y2, and P2Y4 receptors. J. Invest. Dermatol. 120, 440–447.
Corriden, R., Insel, P.A., 2010. Basal release of ATP: an autocrine–paracrine mechanism for cell regulation. Sci. Signal. 3, re 1.
Crosera, M., Bovenzi, M., Maina, G., Adami, G., Zanette, C., Florio, C., Larese, F.F., 2009. Nanoparticle dermal absorption and toxicity: a review of the literature. Int. Arch. Occup. Environ. Health 82, 1043–1055.
Dixon, G.J., Bowler, W.B., Littlewood-Evans, A., Bilbe, G., Sharpe, G.R., Gallagher, J.A., 1999. Regulation of epidermal homeostasis through P2Y2 receptors. Br. J. Pharmacol. 127, 1680–1686.
Donaldson, K., Tran, L., Jimenez, L.A., Duffin, R., Newby, D.E., Mills, N., MacNee, W., Vicki Stone, V., 2005. Combustion-derived nanoparticles: a review of their toxicology following inhalation exposure. Part. Fibre Toxicol. 2 (10), http://dx.doi.org/10.1186/1743-8977-2-10.
Dubyak, G.R., el-Moatassim, C., 1993. Signal transduction via P2-purinergic receptors for extracellular ATP and other nucleotides. Am. J. Physiol. 265, C577–C606.
Elder, J.T., Fischer, G.J., Lindquist, P.B., Bennett, G.L., Pittelkow, M.R., Coffey R.J.Jr., Ellingsworth, L., Derynck, R., Voorh, J.J., 1989. Overexpression of transforming growth factor alpha in psoriatic epidermis. Science 243, 811–814.
Farrar, M.A., Schreiber, R.D., 1993. The molecular cell biology of interferon-gamma and its receptor. Annu. Rev. Immunol. 11, 571–611.
Ferrari, D., Chiozzi, P., Falzoni, S., Dal Susino, M., Melchiorri, L., Baricordi, O.R., Di Virgilio, F., 1997. Extracellular ATP triggers IL-1 beta release by activating the purinergic P2Z receptor of human macrophages. J. Immunol. 159, 1451–1458.
Fitz, J.G., 2007. Regulation of cellular ATP release. Trans. Am. Clin. Climatol. Assoc. 118, 199–208.
Gallucci, R.M., Sloan, D.K., Heck, J.M., Murray, A.R., O'Dell, S.J., 2004. Interleukin 6 indirectly induces keratinocyte migration. J. Invest. Dermatol. 122, 764–772.
Greig, A.V.H., Linge, C., Terenghi, G., McGrouther, D.A., Burnstock, G., 2003. Purinergic receptors are part of a functional signaling system for proliferation and